KU LEUVEN

This document contains the **post-print pdf-version** of the referred paper:

"**Thermal inactivation of *Listeria monocytogenes* in the Shaka agitated reciprocal retort: Influence of food matrix rheology and fat content**"

By *Davy Verheyen, Ozan Altin, Dagbjørn Skipnes, Ferruh Erdogdu,Torstein Skåra, and Jan F. Van Impe*

which has been archived on the university repository Lirias (https://lirias.kuleuven.be/) of the Katholieke Universiteit Leuven.

The content is identical to the content of the published paper, but without the final typesetting by the publisher.

The journal and the original published paper can be found at:
https://www.sciencedirect.com/science/article/pii/S0960308520305344

The corresponding author can be contacted for additional info.

Conditions for open access are available at:
http://www.sherpa.ac.uk/romeo/

Thermal inactivation of *Listeria monocytogenes* in the Shaka agitated reciprocal retort: Influence of food matrix rheology and fat content

Davy Verheyen[a,b,c], Ozan Altin[d], Dagbjørn Skipnes[e], Ferruh Erdogdu[d], Torstein Skåra[e],

Jan F. Van Impe[a,b,c]

[a]BioTeC+ - Chemical and Biochemical Process Technology and Control, KU Leuven,

Gebroeders de Smetstraat 1, 9000 Gent, Belgium

[b]OPTEC, Optimization in Engineering Center-of-Excellence, KU Leuven, Belgium,

[c]CPMF[2], Flemish Cluster Predictive Microbiology in Foods - www.cpmf2.be

[d]Department of Food Engineering, Ankara University, Golbası Kampusu, 06830 Golbası-

Ankara, Turkey

[e]Nofima, P.O. Box 8034, 4068 Stavanger, Norway

davy.verheyen@kuleuven.be, altinozan92@gmail.com, dagbjorn.skipnes@nofima.no,

ferruherdogdu@yahoo.com, torstein.skara@nofima.no, jan.vanimpe@kuleuven.be

Declarations of interest: none

Correspondence to:

Prof. J. F. M. Van Impe

Chemical and Biochemical Process Technology and Control (BioTeC+)

Department of Chemical Engineering, KU Leuven

Gebroeders de Smetstraat 1, B-9000 Gent (Belgium)

jan.vanimpe@kuleuven.be

Tel: +32-16-32.14.66

ABSTRACT

The effect of food matrix rheology and fat content on thermal inactivation of *Listeria monocytogenes* in the Shaka agitated retort (final retort temperatures of 59, 64, and 69°C) was investigated using four fish-based artificial food model systems: low-viscosity liquid (liquid), high-viscosity liquid (xanthan), and emulsions containing 10% and 20% fat (emulsion 10% and emulsion 20%). Model system rheology, quantified by the consistency index K and the flow behaviour index n, influenced the thermal load to which the systems were exposed during treatments. Thermal loads followed the order liquid ≥ emulsion 10% ≥ emulsion 20% ≥ xanthan, a trend which was also valid for the sublethal injury induced to the cells. Log reductions followed the order liquid ≥ emulsion 10% ≥ xanthan ≥ emulsion 20%, indicating a protective effect of an increased fat content, not related to heat transfer differences. Between approximately 59 and 62°C, the temperature range over which the largest portion of the inactivation was achieved, the maximum specific inactivation rate k_{max} followed the same trend as the log reductions. Overall, the effect of food matrix rheology on inactivation efficacy could be linked to heat transfer dynamics, while the effect of fat content was more complex.

Keywords: Food safety, thermal processing, food model systems, food microstructure, predictive microbiology.

1 INTRODUCTION

Thermal processing (pasteurisation or sterilisation) remains the most reliable and most-used method in the food industry for the inactivation of pathogens in/on food products (Pratap Singh et al., 2018). In the thermal processing category, canning processes, involving the use of static retorts (using e.g., steam, water, steam/air, raining and spray water) to heat foods in hermetically sealed containers, have shown to be a convenient and economic way to provide safe and shelf-stable foods (Ates et al., 2014; Erdogdu et al., 2018a; Pratap Singh et al., 2017a). However, suboptimal control of the heating process and the limited knowledge concerning inactivation kinetics of microorganisms often result in the use of thermal processes with excessive microbiological safety margins (Smelt and Brul, 2014). These excessive processes negatively influence food product quality due to nutrient degradation and (permanent) changes to sensory attributes (Awuah et al., 2007).

For liquid food products over a broad viscosity range (e.g., soups, meat in gravy, sauces, possibly also containing particles), the detrimental effects of thermal canning processing can be reduced by using agitated thermal processes, promoting heat transfer by forced convection. Most conventional agitation processes can be classified as end-over-end or axial rotation, with the symmetrical axis of the containers along and perpendicular to the plane of rotation, respectively (Pratap Singh et al., 2018). For both types of rotation, forced convection is caused by an interaction of gravitational and centrifugal forces (Erdogdu et al., 2017; Pratap Singh et al., 2017a; Ramaswamy and Marcotte, 2005; Sarghini and Erdogdu, 2016). Recently, processes involving reciprocal agitation have gained more interest following the development of Shaka

and Gentle Motion retorts (Clifcorn et al., 1950; Dwivedi and Ramaswamy, 2010; Erdogdu et al., 2016; Pratap Singh et al., 2018). Due to the combination of gravity and horizontal acceleration, heat transfer rates of reciprocal agitation processes are considerably higher than for rotational agitation processes (Walden and Emanuel, 2010). The Shaka process involves rapid agitation rates higher than 1 Hz and is suitable for liquid-only foods over a broad viscosity range, while the Gentle Motion process involves slower agitation rates and is more suitable for liquid-particulate foods (Pratap Singh and Ramaswamy, 2016).

Due to the novelty of the technique, there is a need for an improved understanding of parameters influencing heat transfer and microbial inactivation kinetics during reciprocal agitation thermal processes, both in relation to process operating parameters and food product related properties. Over the last decade, the influence of process operating parameters has already been studied rather extensively, e.g., reciprocation intensity and amplitude (Erdogdu et al., 2016; Pratap Singh and Ramaswamy, 2015, 2016), container placement orientation inside the retort (Pratap Singh and Ramaswamy, 2015), and container headspace (Pratap Singh and Ramaswamy, 2015; Pratap Singh et al., 2017b). Concerning food product related parameters, the influence of particle properties (e.g., size, shape, density) in particulate mixtures has been investigated to some extent (Cariño-Sarabia and Vélez-Ruiz, 2013; Singh and Ramaswamy, 2015), but research towards the influence of factors related to microstructural aspects of liquid food products has been scarce. This limited amount of research is striking, since food microstructure, defined as "the spatial arrangement of the structural elements (of a food product) and their interactions" (Heertje, 2014), is known to exert a considerable influence on thermal

inactivation kinetics of foodborne pathogens (Velliou et al., 2013; Wilson et al., 2002). In this regard, food product rheology (e.g., viscosity) and the presence of fat droplets, and in relation to this, the fat content, are prominent examples of microstructural factors which significantly affect heat transfer rates and microbial inactivation kinetics in liquid food products (Chhabra et al., 1999; Fain et al., 1991; Juneja et al., 2001; Oliveira et al., 2018; Schultze et al., 2007; Sheridan and Shilton, 2002; Velliou et al., 2013). Concerning the role of food product rheology in reciprocal agitation thermal processes on the one hand, mathematical models have already been developed to determine the optimal reciprocation rate as a function of product viscosity (Erdogdu et al., 2016, 2017; Pratap Singh and Ramaswamy, 2016). The resulting influence on microbial inactivation kinetics, however, was not taken into account in those studies. On the other hand, the influence of fat droplet presence and fat content on heat transfer and microbial inactivation in reciprocal agitation retort systems has, to the best knowledge of the authors, thus far not been investigated.

While novel food processing technologies are traditionally validated using artificially inoculated foods (NACMF, 2010), a general trend towards the use of food model systems that simulate, to a certain degree, the compositional and microstructural properties of the food products of interest is observed in recent years (Baka et al., 2017). Advantages related to the use of food model systems instead of real food products for experimental research include (i) a reduction in experimental workload, (ii) increased reproducibility, (iii) the absence of background microflora, and (iv) the possibility to systematically study independent factors (Baka et al., 2016). Concerning reciprocal agitation thermal processes, however, most studies related to the influence of food product parameters (e.g., rheology) on heat transfer were solely conducted in

model systems which were not closely related to the composition and microstructure of relevant food products, e.g., distilled water (Erdogdu et al., 2016), carboxymethylcellulose (Singh and Ramaswamy, 2015), and glycerine (Pratap Singh et al., 2015; Pratap Singh and Ramaswamy, 2015, 2016). Using artificial food model systems with compositional and microstructural properties more closely related to relevant food products, would improve applicability of findings for the food industry. In addition, these more relevant model systems would allow studies involving pathogenic bacteria, elucidating the impact of reciprocal agitation processes on food safety. The work of Ates et al. (2014, 2017), in which the inactivation of *Listeria innocua* (i.e., a non-pathogenic surrogate for *L. monocytogenes*) was investigated in a fish soup model system, marked a first step in this promising direction, also being the only research (to the best knowledge of the authors) in which microbial inactivation during reciprocal agitation thermal process was experimentally validated.

In this study, the influence of food matrix rheology and fat content on bacterial inactivation in the Shaka reciprocal agitation retort system was investigated using artificial food model systems. Model system composition was based on processed fish products (e.g., fish soup, fish sauce, fish salad), while major food microstructural elements of such products were also present in the model systems (e.g., fat droplets, relatively high viscosity). Processed fish products were selected as a food product category, since these are commonly subjected to thermal processing (Rosnes et al., 2011). The heat load required for the inactivation of pathogenic microorganisms is often detrimental for the quality of processed fish products (e.g., dry structure, flaking), explaining their relevance for novel thermal processing technologies which involve shorter heating times at reduced temperatures (Skåra et al. 2002). As a target

microorganism, the bacterium *Listeria monocytogenes* was selected because of (i) its prevalence in processed fish products, (ii) its high heat resistance compared to other non-sporulating bacteria, and (iii) its common use as a target microorganism for the design of thermal inactivation treatments (Ben Embarek, 1994; Farber and Peterkin, 1991; Rosnes et al., 2011).

2 MATERIALS AND METHODS

2.1 Experimental design

Experiments were conducted using fish-based food model systems varying in rheology and fat content. In order to allow a systematic investigation of the influence of food matrix fat content and rheology on bacterial inactivation, the model systems exhibited minimal variation in compositional and physicochemical factors (Verheyen et al., 2018, 2020a). The model systems were inoculated with a *L. monocytogenes* strain cocktail and subjected to Shaka treatments at three different temperatures (i.e., 59, 64, and 69°C), using three different treatment times at each temperature. Log reductions and sublethal cell injury following each individual treatment were calculated, and temperature evolution inside the model systems was recorded during each treatment. In order to enable an estimation of thermal inactivation parameters during a typical Shaka process, the two shortest treatments were considered as intermediate sampling points for the longest treatment and a mathematical model was fitted to the entire dataset for each model system. This approach was used because estimating inactivation parameters solely based on data from one treatment time at each temperature (i.e., only initial and final cell density available) would not be accurate. The influence of food matrix rheology and fat content on bacterial inactivation was investigated by comparing log reductions, inactivation rates and sublethal injury percentages among the different model systems. For this purpose, rheological properties of the model systems were also quantified.

2.2 Model system preparation

The model system preparation procedure was based on the protocol of Verheyen et al. (2018). The four different model systems used were (i) a low-viscosity liquid (liquid), (ii) a high-viscosity liquid (xanthan), (iii) an emulsion containing 10% fat (emulsion 10%), and (iv) an emulsion containing 20% fat (emulsion 20%). An overview of the composition and physicochemical properties (i.e., density, pH, and a_w) of the model systems is provided in Table 1 and **Supplementary Material 1**, respectively. Fat droplet size of the two emulsion model systems was evenly distributed around 1 μm (Verheyen et al., 2018).

Model systems were divided over PP beakers with a LDPE screw lid (52 mm inner diameter $\times$ 74 mm height, VWR International, Leuven, Belgium). Beakers were filled up to 90% of their total height (i.e., approximately 129-136 g, depending on the model system due to the differences in density), resulting in a head space of 10%. Since the container head space significantly affects heat transfer in agitated retort systems (Pratap Singh et al., 2018), an identical head space percentage was used for all model systems.

2.3 Rheological characterisation

Rheological measurements were conducted using a Discovery Hybrid Rheometer (DHR-2, TA Instruments, New Castle, DE, USA), equipped with a 40-mm parallel plate system, consisting of a crosshatched upper and lower plate. The gap size between the two plates was set at 500 µm. Temperature control was regulated by means of a Peltier temperature control system and upper heated plate. The model systems were analysed by means of their steady-state behaviour over a temperature

range from 20 to 70°C, as described in Verheyen et al. (2020b). Briefly, model

systems were prepared 24 h prior to measurement, and were loaded onto the bottom

plate (1.6 mL per sample) after which a delay of 2 min was set. The shear rate was

increased linearly from 0.01 to 50.00 Hz, and the corresponding shear stress after the

sample reached the steady-state was evaluated. The relationship between the shear

stress and shear rate was characterised by Equation 1, which represents the power law

model (Reiner, 1926).

$$\tau = K \cdot \dot{\gamma}^n \tag{1}$$

With τ [Pa], the shear stress; $\dot{\gamma}$ [1/s], the shear rate; K [Pa/s], the consistency index;

and n [−], the flow behaviour index representing the extent of deviation from

Newtonian behaviour. Both model parameters (i.e., K and n) were estimated by fitting

a power function to the experimental data using Microsoft Excel (Microsoft

Corporation, WA, USA). This procedure was conducted at five temperatures (i.e.,

20.0, 32.5, 45.0, 57.5, and 70°C), resulting in a characterisation of the rheological

behaviour of the model systems over the relevant temperature range. Experiments

were conducted independently in duplicate.

2.4 Microorganisms and inoculation procedure

L. monocytogenes strains LMG 23773, LMG 23774, and LMG 26484 were acquired

from the BCCM/LMG bacteria collection of Ghent University in Belgium

(https://bccm.belspo.be/). The strains originated from fish-based food products, i.e.,

smoked salmon (LMG 23773 and LMG 23774) and tuna salad (LMG 26484). Stock

cultures were stored at −80°C in Brain Heart Infusion Broth (Merck Millipore,

Darmstadt, Germany) and 20% (v/v) glycerol (Acros Organics, NJ, USA). Separate

purity plates were prepared for each strain by spreading a loopful of the respective stock culture onto a BHI Agar plate (Merck Millipore, Darmstadt, Germany). After incubation at 30°C for 24 h, one colony of each plate was transferred to 20 mL of BHI broth in separate 50 mL Erlenmeyers. Inoculated Erlenmeyers were incubated at 30°C for 24 h, after which 20 µL of the medium was transferred to fresh Erlenmeyers containing 20 mL of BHI broth. These were again incubated at 30°C for 24 h, resulting in stationary-phase $L.\ monocytogenes$ cultures with a cell density of approximately 10^9 CFU/mL for each strain. Equal-volume aliquots of each strain were mixed, resulting in a three-strain $L.\ monocytogenes$ cocktail with a cell density of approximately 10^9 CFU/mL.

Model systems were homogeneously inoculated with the $L.\ monocytogenes$ strain cocktail to a cell density of approximately 10^8-10^9 CFU/mL, based on the protocol of Verheyen et al. (2019). For each beaker containing one of the model systems (i.e., liquid, xanthan, emulsion 10%, emulsion 20%), 30 mL of the strain cocktail was transferred to a 50 mL falcon tube and centrifuged at 18,500 g for 15 min at 4°C. The supernatant was carefully removed and 5 mL of model system was transferred from the beaker containing the model system to the falcon tube containing the pellet, using a 1 mL viscous pipet (Microman, Gilson, France). The pellet was detached from the edge of the falcon tube using an inoculation loop, after which the pellet was homogeneously distributed over the 5 mL of model system by vortex mixing for 2 min. The inoculated fraction of the model system was transferred back to the original beaker, which was subsequently shaken thoroughly in order to ensure an even distribution of the $L.\ monocytogenes$ cells. The inoculated model systems were stored

at 10°C for approximately 16 h prior to the inactivation experiment. The entire

inoculation procedure was conducted under aseptic conditions.

2.5 Shaka treatment

Thermal inactivation experiments were conducted in a 911 EAT Shaka retort

(Steriflow, Roanne, France). A simplified schematic overview of the Shaka system is

provided in Figure 1. In brief, the temperature inside the retort is regulated by means

of raining water and/or steam. A preheating tank is present to supply hot water to the

retort at the start of the process. The pressure inside the retort (and the preheating

tank) is regulated via pressurized air inlets.

The processing conditions of the Shaka treatments were selected based on the study of

Ates et al. (2014). Prior to every inactivation process, the water in the preheating tank

was heated to 50°C. Inactivation processes consisted of five phases, i.e., (i) filling

phase, the retort was filled with the preheated water; (ii) heating phase, the water in

the retort was heated to the target temperature for the respective inactivation

experiment while the retort was agitated at 80 strokes per minute (spm); (iii) holding

phase, the temperature of the retort water was kept constant at the target temperature

while the retort was agitated at 100 spm; (iv) cooling phase 1, the retort water was

cooled to 30°C while the retort was agitated at 100 spm; and (v) cooling phase 2, the

retort water was cooled to 20°C while the retort was agitated at 80 spm. More

information (e.g., time, overpressure) concerning the different steps of the inactivation

processes is provided in Table 2. A limited overpressure (i.e., maximum 0.4 bar) was

applied to maintain the structural integrity of the sample containers (Wedding et al.,

2007).

Thermal inactivation experiments were conducted at three different holding phase temperatures (i.e., 59, 64, and 69°C) and for three different holding phase time periods at each temperature. Based on preliminary experiments, the longest treatment times were selected to accomplish an approximate 6 log reduction of *L. monocytogenes* in the liquid system. An overview of the duration of the different treatments is provided in Table 3. Prior to each inactivation experiment, three independent replicates (i.e., each independently inoculated with individual replicates of the strain cocktail) of each model systems inoculated with *L. monocytogenes* were placed horizontally into the retort chamber. The beakers were kept in position using vertically-placed PTFE plates with evenly-distributed holes. After each inactivation treatment, the Shaka retort was drained. The beakers were removed from the retort and kept in an ice-water bath prior to analysis.

2.6 Microbiological analysis

For all samples, serial decimal dilutions were prepared using a 0.90% (w/v) NaCl solution and plated on BHI agar and PALCAM agar (PALCAM *Listeria* Selective Agar, according to Van Netten et al. (1989), Merck Millipore, Darmstadt, Germany) using the drop technique (Herigstad et al., 2001). While drops of 20 µL were plated for dilutions 10^{-1} to 10^{-6}, drops of 100 µL (spread out using an L-shaped cell spreader) were plated for the undiluted sample to acquire a lower detection limit (DL). Due to the viscous nature of the model systems, pipetting of the undiluted samples during the microbiological analysis (e.g., diluting, drop-plating) was conducted using a viscous pipette (Microman, Gilson, France). Plates were incubated for 30 to 48 h at 30°C prior to enumeration. Cell counts were considered significant when at least 10 colonies per

two drops of 100 µL were detected for the undiluted sample, resulting in a DL of 1.7 log (CFU/mL).

2.7 Log reduction calculation

Log reductions were calculated based on average log-transformed counts before and after each treatment. When cell densities below the DL were detected following the treatment, these cell densities were considered equal to the DL (i.e., 1.7 log CFU/mL) in order to estimate a minimum log reduction.

2.8 Temperature measurements

Preliminary experiments revealed that the temperature gradient in the beakers containing the model systems during the Shaka treatments was insignificant. Temperature evolution inside the model systems was characterised over the course of the Shaka treatments at the different temperatures. For the treatment at a holding temperature of 59°C, preliminary experiments revealed that a constant temperature was reached inside the model systems before the first sampling point. Therefore, temperature over the course of the treatments at 59°C was only recorded for the longest treatment time, and temperature profiles for shorter treatment times were constructed by shortening the holding time of the longest treatment. TrackSense Mini Loggers (Ellab, Roedovre, Denmark) were attached to the lid of the beakers, enabling temperature measurements at a beaker height of approximately 58.0 mm. Temperature was recorded every second and data was processed using the ValSuite Pro software (Ellab, Roedovre, DK). Temperature measurements were performed independently in duplicate.

In order to quantify the amount of heat transfer inside the different model systems during the Shaka treatments, the thermal load to which the cells were exposed was calculated by integrating the different temperature profiles over time ($\int T dt$). For this purpose, only the heating and holding phase were taken into account.

2.9 Sublethal injury assessment

Sublethal injury (SI) was calculated according to the formula of Busch and Donnelly (1992), as illustrated by Equation 2.

$$SI = \left(1 - \frac{\text{CFU on selective agar}}{\text{CFU on nonselective agar}}\right) \cdot 100\% \tag{2}$$

BHI agar and PALCAM agar served as a nonselective and selective plating medium, respectively, with the former supporting cell recovery. Using Equation 2, it is assumed that nonselective media represent both uninjured and injured microorganisms, while selective media only represent uninjured (target) microorganisms (Noriega et al., 2013). If counts below the DL were detected on PALCAM agar, these counts were assumed to be equal to the DL, enabling the calculation of a minimum amount of SI. If counts below the DL were detected on BHI agar, calculation of SI was not possible.

2.10 Estimation of thermal inactivation kinetics

Thermal inactivation was modelled for the longest treatment time at each temperature (i.e., holding times t_h of 37.5, 13.4, and 8.8 min for treatments at holding temperatures T_h of 59, 64, and 69°C, respectively), enabling the estimation of kinetic parameters over the course of the Shaka process, and the comparison of those parameters among the different model systems. Based on the protocol of Verheyen et al. (2019, 2020b),

thermal inactivation was modelled using the dynamic form of the model of Geeraerd et al. (2000), extended with a Bigelow-type temperature relation (Garre et al., 2017; Stumbo, 1973) in order to take the actual temperature inside the model systems into account. It was assumed that the inactivation rate was equal to zero for temperatures lower than 50°C, since, in the absence of additional stresses, *L. monocytogenes* is not inactivated at these temperatures (Valdramidis et al., 2006b). Model parameters were estimated from the set of experimental data via the minimisation of the sum of squared errors, using the lsqnonlin routine of the Optimisation Toolbox of MatLab® version R2018b (The Mathworks Inc., Natick, USA). For each model system, the differential equations of the inactivation model were solved simultaneously for the inactivation data at 59, 64, and 69°C, using the MatLab solver ode45. Standard errors of parameter estimates were calculated from the Jacobian matrix. A global estimation procedure was standardised for all replicates for each model system. The model of Geeraerd et al. (2000) and the Bigelow-type relation (Garre et al., 2017; Stumbo, 1973) are represented by Equation 3 and 4, respectively.

$$\frac{\mathrm{d}N(t)}{\mathrm{d}t} = -k_{max} \cdot \left(1 - \frac{N_{res}}{N(t)}\right) \cdot N(t) \tag{3}$$

$$k_{max}(T) = \begin{cases} k_{max}(T_{ref}) \cdot 10^{\frac{T-T_{ref}}{z}}, & \text{if } T \geq 50°C \\ 0, & \text{if } T < 50°C \end{cases} \tag{4}$$

With N [CFU/mL], the cell density at time t; N_{res} [CFU/mL], the residual cell density; k_{max} [1/min], the maximum specific inactivation rate; T [°C], the core-temperature of the model system; T_{ref} [°C], the reference temperature; $k_{max}(T_{ref})$ [1/min], the maximum specific inactivation rate at the reference temperature; and z [°C], representing the sensitivity of k_{max} to temperature changes. The initial cell density N_0 [CFU/mL], included in the model via the left-hand side of Equation 3, was imposed to

be equal to the average of the measured cell densities at time zero; giving too much "freedom" to this parameter would be detrimental for the model accuracy due to the absence of sampling points during the early treatment stages. Datta (1993) stated that the selected reference temperature should be close to the maximum temperature achieved in the systems. Based on preliminary trials, a reference temperature T_{ref} equal to 59°C was therefore selected. Values from lab-scale experiments (i.e., in water baths, involving a short come-up time of approximately 2 min) for k_{max}(59°C) and z, obtained by Verheyen et al. (2019, 2020b) for the *L. monocytogenes* strain cocktail in the four relevant model systems, were used as initial estimates for the respective parameters during the modelling procedure. The reader is referred to the works of Geeraerd et al. (2000) and Garre et al. (2017) for a more detailed explanation (and practical relevance) of the model parameters.

L. monocytogenes cell densities were only recorded after cooling steps, during which inactivation took place as long as the temperature inside the model systems was higher than 50°C. In order to be able to use the cell densities following the shorter treatment times at each treatment temperature as intermediate sampling points for the longest treatment time at that temperature, a theoretical cell density prior to cooling N_i* was estimated for each treatment time. In brief, only the fraction of the estimated log reduction which was caused by the heating and holding phase of the Shaka process was taken into account to calculate N_i*, using a reduction factor (1-red_{cool}/red_{total}) which represents this fraction. The log reduction during a certain period of the Shaka treatment (i.e., during cooling and during the total process, needed to calculated red_{cool} and red_{total}, respectively) is obtained by dividing the F value at the reference temperature by the D value at the reference temperature (Berk, 2013). The

D value at the reference temperature can be calculated as $\ln 10 / k_{max}(T_{ref})$ (Garre et al., 2017). The formulas for the calculation of *red* (i.e., the log reduction contributions necessary to calculate the reduction factor) and N_i^* are represented by Equation 5 and 6, respectively. The right-hand side of Equation 6 represents a simplified form of the equation; the complete mathematical deduction is not shown.

$$red_{cool\,or\,total} = \frac{F_{59°C}}{D_{59°C}} = \frac{F_{59°C} \cdot k_{max}(59°C)}{\ln 10} = \tag{5}$$

$$\frac{\int_{t_{a(\prime)}}^{t_b} 10^{\frac{T-T_{ref}}{z}} dt \cdot k_{max}(59°C)}{\ln 10}$$

$$N_i^* = N_0^{avg} - \left(1 - \frac{red_{cool}}{red_{total}}\right) \cdot \left(N_0^{avg} - N_i\right) = N_0^{avg} - \left(1 - \right.$$

$$\left. \frac{\int_{t_{a\prime}}^{t_b} 10^{\frac{T}{z}}}{\int_{t_a}^{t_b} 10^{\frac{T}{z}}}\right) \cdot \left(N_0^{avg} - N_i\right) \tag{6}$$

With N_i^* [CFU/mL], the theoretical cell density prior to cooling; N_0^{avg} [CFU/mL], the average cell density at time 0 for the untreated sample; N_i [CFU/mL], the measured cell density following cooling; red_{cool} [log CFU/mL], the estimated log reduction during the cooling phases; red_{total} [log CFU/mL], the estimated log reduction during the total process; $F_{59°C}$ [min], the F value at 59°C, representing the theoretical treatment time at a constant temperature of 59°C required to achieve a certain log reduction; $D_{59°C}$ [min], the time necessary to reduce the number of bacteria by one log unit under isothermal conditions at 59°C; z [°C], the temperature increase necessary for a 10-fold reduction of the D value; t_a [min] (represented as t_a for the total process, $t_{a\prime}$ for the cooling), the time point at which the temperature first exceeds 50°C for the given treatment period; and t_b [min] (represented as t_b for both the total and cooling process, since the end time was the same for both), the time point at which the temperature drops below 50°C for the given treatment period. The z values

for the *L. monocytogenes* strain cocktail in the four different model systems were obtained from lab scale experiments, i.e., in water baths, involving a short come-up time of approximately 2 min (Verheyen et al., 2019; 2020b).

For each model system and treatment temperature, a dataset of five time points was used, consisting of three independent replicates at each time point. The log-transformed cell densities at time zero were used in their original form. Cell densities obtained after the three different treatments were adjusted in order to exclude the inactivation caused during the cooling phases, and the cooling time was subtracted from the original total times, resulting in the three middle time points. The fifth (and last) time point was formed by using the obtained cell density after the longest treatment time including cooling phases, but the time was adapted to the last time during the cooling phase at which inactivation took place (i.e., where the temperature was still above 50°C). Consequently, an overestimation of the tailing phase duration was avoided. In general, counts below the DL were assumed to be equal to the DL, in order to avoid an overestimation of the inactivation following the Shaka process.

2.11 Statistical analysis

Significant differences between model parameters were determined using analysis of variance (ANOVA, single variance) test at a 95.0% confidence level ($\alpha = 0.05$). Fisher's Least Significant Difference (LSD) test was used to distinguish which means were significantly different from others. Standardised skewness and standardised kurtosis were used to assess if data sets came from normal distributions. The analyses were performed using Statgraphics Centurion XVII Package (Statistical Graphics, Washington, USA). Test statistics were regarded as significant when $P \leq 0.05$.

3 RESULTS AND DISCUSSION

3.1 Rheological characterisation

Table 4 shows the rheological properties of the different model systems, according to

the power law model (Reiner, 1926). The consistency index K is a measure of the

viscosity of non-Newtonian fluids and the flow behaviour index n represents the

extent of deviation from Newtonian behaviour, with Newtonian fluids being

characterised by $n = 1$. In general, K decreased with increasing temperature, while no

clear correlation between temperature and n was observed. Similar trends are

commonly reported in literature for various liquid food systems (Chhinnan et al.,

1985; Maskan and Göğüş, 2000; Sopade and Filibus, 1995; Vitali and Rao, 1984).

Both for K and n, there was a clear correlation among the different model systems at

each temperature, following the order K (emulsion 20%) > K (emulsion 10%) $\geq K$

(xanthan) $\geq K$ (liquid), and n (liquid) > n (xanthan) $\geq n$ (emulsion 10%) $\geq n$ (emulsion

20%). A constant relationship between the rheological properties of the different

model systems over the entire temperature range was hence revealed. In addition, the

flow behaviour index n was smaller than 1 for all model systems, indicating pseudo-

plastic or shear-thinning behaviour.

3.2 Thermal load

The temperature evolution in the different model systems over the course of the

different Shaka treatments at 59 and 64°C is illustrated in **Supplementary Materials**

2 and 3, while the evolution at 69°C (i.e., the case where the most prominent

differences can be seen among the model systems) is illustrated in Figure 2. The

thermal loads of the model systems during the different Shaka treatments are provided

in Table 5. In general, the thermal load was the highest in the liquid system and the lowest in the xanthan system. The two emulsion systems exhibited intermediate behaviour and were only significantly different for one condition (i.e., 64°C for 10.4 min).

Due to the forced convection of the model systems during Shaka treatment, convective heat transfer is dominant over conductive heat transfer (Erdogdu et al., 2017). The high thermal load inside the liquid system was therefore probably caused by the lower consistency index K (i.e., representing a lower viscosity) in comparison to the other systems. Solely based on K, however, thermal loads would be expected to follow the order liquid $\geq$ xanthan $\geq$ emulsion 10% > emulsion 20%. Therefore, the deviation from Newtonian behaviour (i.e., represented by the flow behaviour index n) probably also exerted an influence on heat transfer rates. Forced convection heat transfer is facilitated in shear-thinning fluids (i.e., $n < 1$) and more with increasing shear-thinning behaviour (Bharti et al., 2007, 2008). Since the flow behaviour index n was lower in the emulsion 20% than in the emulsion 10%, the effect of the higher consistency index K in the emulsion 20% was probably cancelled out. Consequently, the relation of thermal loads among the different model systems was the result of the opposite trends in K and n among the different model systems. While the lowest thermal loads in the xanthan system could also be related to the higher n in this system, the large amount of air bubbles that was observed in this system following Shaka treatments possibly also exerted an important effect. These bubbles may have disrupted the flow of the xanthan system, hindering convective heat transfer even further.

A comparison of the thermal conductivity values of the different model systems (Erdogdu et al., 2018b; Verheyen et al., 2020b) revealed that thermal conductivity in the two emulsions was significantly lower than in the liquid and xanthan system. In addition, no significant differences in thermal conductivity were observed between the emulsion 10% and emulsion 20%. While these results are in line with those obtained for the thermal load, their influence was probably insignificant due to the dominance of convective heat transfer during Shaka treatments.

3.3 Thermal inactivation of *Listeria monocytogenes*

3.3.1 Log reduction

An overview of the *L. monocytogenes* log reductions following the different Shaka treatments is provided in Table 6. Log reductions which approximate a total inactivation of all *L. monocytogenes* cells were only observed in the liquid (at 59, 64 and 69°C) and the emulsion 10% (59°C). When inactivating *Listeria innocua* in liquid model fish soup samples using the Shaka retort (Ates et al., 2014), similar log reductions where obtained following less severe holding time-temperature combinations (i.e., 62°C-11.5 min, 65°C-6.8 min, 68°C-5.5 min), probably caused by the absence of thickening agents (e.g., xanthan gum and sodium alginate, as used in the current study) in the fish soup.

As a general trend over all conditions in the current study, log reductions followed the order liquid ≥ emulsion 10% ≥ xanthan ≥ emulsion 20%. A comparison of the log reductions obtained in the different model systems with the respective calculated thermal loads (Table 5) reveals a certain relation between the two parameters, although a direct correlation was not seen in all cases. On the one hand, the log

reductions in the emulsion 20% were often lower than expected from the thermal load values, since thermal loads in the emulsion 10% and emulsion 20% were in general not significantly different. While this phenomenon could be observed at all temperatures, with log reductions always being lower in the emulsion 20% than in the emulsion 10%, significant differences were only seen at 59 and 69°C. On the other hand, the log reductions in the xanthan system were higher than expected from the thermal load values, with log reductions never being significantly lower than in the emulsion 20% which, in most cases, was exposed to higher thermal loads. In essence, these two phenomena can be simplified to a protective environment for the cells in the emulsion 20% which was not expected solely based on the thermal load values. Consequently, an increased food matrix fat content (i.e., emulsion 20% vs. emulsion 10%) seemed to result in additional protective effects against thermal inactivation for the *L. monocytogenes* cells. However, it should be taken into account that food matrix fat content also influenced the rheological properties of the model systems. In addition, it should be taken into account that the thermal load was only calculated based on the temperature in the centre of the model system. However, inhomogeneous temperature distributions may have been present in the model systems, especially in the more viscous systems. In those cases, bacterial log reductions cannot be accurately linked to the measured thermal loads in the centre of the model systems, since inactivation would be more prominent at locations at temperatures higher than the core temperature. Measuring the temperature at different locations in the model systems, possibly in combination with advanced mathematical modelling techniques to get a complete view of the temperature distribution (e.g., as conducted by Erdogdu et al. (2017)), would contribute to an improved understanding of the inactivation behaviour of *L. monocytogenes* in the different model systems.

3.3.2 Sublethal injury assessment

Table 7 shows the sublethal injury (SI) of *L. monocytogenes* following the different

Shaka treatments. When statistical differences were observed, SI was always the

highest in the liquid and the smallest in the xanthan system. The two emulsions

exhibited an intermediate behaviour between these two limits, with SI in the emulsion

20% only being significantly lower than in the emulsion 10% in three conditions (i.e.,

59°C for 37.5 min, 64°C for 13.4 min, and 69°C for 8.8 min).

A similar trend was observed for the log reductions, indicating that the amount of SI

of *L. monocytogenes* was closely related to the log reductions. Hence, more effective

thermal treatments generally also resulted in more SI.

Since SI percentages below 70-80% do not pose severe food safety risk (i.e., log-scale

differences of approximately 0.5 or lower), the higher percentages are of greater

interest. In this regard, maximum SI percentages of 96.7, 80.4, 92.4, and 87.4% were

observed for the liquid, xanthan, emulsion 10% and emulsion 20%, respectively, not

taking into account conditions for which counts below the DL were detected on the

selective medium. Ates et al. (2014) also reported high amounts of SI of *L. innocua* in

their fish soup model systems following Shaka treatments at 62, 65, and 68°C, under

some conditions reaching more than 99%. These findings indicate that the efficacy of

Shaka treatments for the inactivation of *L. monocytogenes* in real food products

should be validated with caution. The background flora present in real food products

necessitates the use of selective media to enumerate the number of bacterial survivors

following Shaka treatments. The growth of sublethally injured cells is (at least partly)

inhibited on selective media due to the sensitivity of the cells to the selective

compounds in the media, (Brashears et al., 2001). When subjected to appropriate

environmental conditions, these sublethally injured cells could recover from their

damage, possibly leading to underestimated contamination levels and the resulting

food safety risks (Noriega et al., 2013). It should, however, also be noted that the

environmental conditions to which cells are exposed in food products can be more

stressing than the favourable growth environment offered by BHI agar. Hence, the

counts on BHI agar, as reported in this study to represent the total population of

injured and uninjured cells, could also be an overestimation of the disease-causing cell

population in real food products.

3.3.3 Estimation of thermal inactivation kinetics

Since intermediate sampling during Shaka treatments is not possible, the cell density

evolution over the course of the longest Shaka treatment was estimated by interpreting

the shorter Shaka treatments as intermediate sampling points. The model of Geeraerd

et al. (2000), extended with a Bigelow-type temperature dependency (Garre et al.,

2017; Stumbo, 1973), was fitted to the experimental data, because the classical

concept of D and z values is unable to deal with the typical non-loglinear behaviour of

survivor curves during mild thermal treatments. The estimated thermal inactivation of

L. monocytogenes in the different model systems during these longest Shaka

treatments is illustrated in Figures 3-5, for treatments at 59, 64, and 69°C,

respectively. Eight different model parameters were estimated, i.e., $k_{max}(T_{ref})$, z,

$N_0(59°C)$, $N_0(64°C)$, $N_0(69°C)$, $N_{res}(59°C)$, $N_{res}(64°C)$, and $N_{res}(69°C)$. An overview

of the estimated parameter values is provided in Table 8, except for the initial cell

densities N_0 (which were imposed to correspond to the measured cell densities at time

zero). For the emulsion 20%, it should be noted that the inactivation phases, based on

which the parameter estimations were conducted, never coincided with temperatures higher than 61°C and that inactivation at temperatures higher than 59°C was in any case very limited. Therefore, the estimated parameters for the emulsion 20% were assessed critically.

The maximum specific inactivation rate at the reference temperature $k_{max}(T_{ref})$ followed a similar trend as for the log reductions for the longest treatment at this temperature (59°C), i.e., highest in the liquid and emulsion 10% (although k_{max} was significantly higher in the liquid than in the emulsion 10%) and lowest in the xanthan and emulsion 20%. The z values followed the trend emulsion 10% ≥ xanthan ≥ liquid ≥ emulsion 20%. Not taking the inaccurate value for the emulsion 20% into account, this trend corresponds to an increasing microbial heat resistance with increasing structural complexity of the model systems. The residual cell populations N_{res} followed the same general trends as the log reductions for the longest treatment times (Table 6), although more significant differences were observed than for the log reductions. As the observed log reductions are a more accurate way of representing the surviving cell populations following the different treatments, the N_{res} values were not discussed in more detail. Concerning the N_{res} parameters, it should also be noted that the presence of a significant N_{res} value is not necessarily linked to surviving cells which are resistant to thermal treatments; it only means that the residual subpopulation of cells survived the particular treatment to which they were exposed. While this survival could be caused by phenomena such as heat resistance and heat adaption, it could also be due to a longer heat treatment being required to inactivate all cells (Geeraerd et al., 2000).

The k_{max} values at 59°C and the z values, obtained for the Shaka treatments, were also compared to lab-scale values obtained for the *L. monocytogenes* cocktail in the studies of Verheyen et al. (2019, 2020b), i.e., in water baths, involving a short come-up time of approximately 2 min. The k_{max} values for the Shaka treatment were significantly lower than those obtained at the lab scale, i.e., 0.394 ± 0.004, 0.421 ± 0.001, 0.339 ± 0.000, and 0.321 ± 0.001, for the liquid, xanthan, emulsion 10%, and emulsion 20%, respectively. The z values for the Shaka treatment were significantly higher than those obtained at the lab scale, i.e., 5.98 ± 0.03, 6.72 ± 0.00, 6.57 ± 0.00, for the liquid, xanthan, and emulsion 10%, respectively (z values for the emulsion 20% were not compared because of the inaccuracy of the model fit at high temperatures). Hence, the *L. monocytogenes* cells were more heat resistant during Shaka treatments than at the lab scale. A similar trend was seen by Bolton et al. (2000) for the inactivation of *L. monocytogenes* NCTC 11994 in minced beef samples treated in a water bath and a static retort. Dynamic temperature profiles which involve a long temperature holding time, as applied in heating retorts, have been reported to result in microbial heat resistance induction (Cattani et al., 2016; Valdramidis et al., 2006a, 2007, 2008), probably due to the formation of heat-shock proteins (Stephens et al., 1994). The obtained parameter values were also compared to those reported for *L. monocytogenes* in different heating menstrua, e.g., milk, broths, diluted soups (Aryani et al., 2015; Mackey and Bratchell, 1989; Sörqvist, 2003). The reported k_{max} values (mainly recalculated from reported D values) ranged from 0.021 to 0.400 and from 0.221 to 3.000 at 55 and 60°C, respectively, while z values ranged from 4.30 to 11.45. Consequently, the parameter values from the current study fall mainly within the more heat resistant range of these reported values, i.e., low k_{max} and high z. The reason for this phenomenon was probably threefold, i.e., (i) the relatively high heat resistance of

the used *L. monocytogenes* strain cocktail, as evidenced by the lab-scale experiments

(ii) the aforementioned induced microbial heat resistance for dynamic temperature

profiles, and (iii) the use of relatively complex model systems in the current study.

Concerning the third explanation, most literature parameter values were obtained in

simple liquid heating menstrua, as compared to the more complex viscous media used

in the current study, possibly also containing high fat content. In this regard, the study

of Juneja et al. (2020) also reported parameter values in the more heat resistant range

for inactivation experiments conducted in ground beef, an even more complex (solid)

food product.

Figure 6 shows the temperature-dependence of k_{max} in the different model systems.

This temperature-dependency is shown up until a temperature of 64°C, because the

inactivation in this study was only scarcely caused by higher model system

temperatures. Due to the nonisothermal nature of the Shaka treatments, k_{max} values at

a certain temperature cannot be directly linked to treatments with similar holding

phase temperatures. For example, *L. monocytogenes* cells during the Shaka treatment

with a holding phase at 64°C will be "subjected" to inactivation rates based on k_{max}

values at temperatures ranging between 50 and 64°C during the entire treatment.

Additionally, since k_{max} values in the emulsion 20% at temperatures higher than 59°C

could not be estimated accurately, these were not taken into account during further

discussion.

At low temperatures, the maximum specific inactivation rate k_{max} followed the trend

emulsion 10% ≥ liquid ≥ xanthan ≥ emulsion 20%, even though differences among

the different model systems were relatively small. Starting from temperatures slightly

below 59°C, k_{max} in the liquid surpassed the one in the emulsion 10% and k_{max}

followed the trend liquid ≥ emulsion 10% ≥ xanthan ≥ emulsion 20%. The latter trend

was similar to the one observed for the log reductions. At approximately 62°C, k_{max} in

the xanthan system surpassed that of emulsion 20%. However, these high

temperatures only contributed to a relatively small portion of the inactivation in these

two model systems, thus explaining their limited influence.

Differences in observed log reductions (Table 6) among the different systems can be

explained based on the k_{max} values (Figure 6) at the different temperatures and the

temperature profiles inside the systems (Figure 2-5 and **Supplementary Materials 2**

and 3). For the treatments with a holding phase temperature of 59°C, the largest part

of the log reduction in all model systems was achieved after the temperature of the

systems had already reached 59°C (as can be seen in Figure 3). Therefore, the

observed log reductions for these treatments followed a similar trend as the k_{max}

values at 59°C. Inactivation profiles were similar in the liquid and emulsion 10% on

the one hand, and in the xanthan system and the emulsion 20% on the other, which

can be explained by the similar k_{max} values at 59°C. For the shortest treatment time at

this temperature (i.e., 22.5 min holding time), the temperature in the model systems

remained below 59°C during a larger fraction of the total treatment, explaining the

relatively low log reductions in the two emulsion systems. This was of particular

importance in the emulsion 20% for which k_{max} at temperatures below 58°C was

considerably lower than in the other systems. For the treatments with a holding phase

temperature of 64°C, the largest part of the log reduction in the liquid system occurred

at temperatures above 59°C, while most of the inactivation occurred below 59°C in

the other model systems. This phenomenon explains why the log reduction in the

liquid system was significantly larger than in the other systems. The quasi-absent log

reductions in the emulsion 20% system at this temperature are again explained by the

very low k_{max} in the system at temperatures below 58°C. For the treatments with a

holding phase temperature of 69°C, similar conclusions can be made as for the

treatments at 64°C.

Overall, the observed log reductions were caused by the combined effect of the heat

transfer differences among the different model systems and the temperature-

dependency of k_{max}, which was also model system specific. Both effects can possibly

be linked to the effect of food matrix viscosity and/or fat content. Increasing the

model system viscosity (i.e., xanthan vs. liquid) resulted in lower heat transfer rates,

in turn leading to a decrease in k_{max}. When comparing the underlying numerical values

(data not shown) of the k_{max} curves of the liquid and xanthan system in Figure 6, it can

be observed that the higher viscosity of the xanthan system result in a k_{max} which was

approximately 20% lower than in the liquid system at 51°C. Similarly, k_{max} in the

xanthan system was approximately 27% lower than in the liquid system at 64°C.

Hence, the decrease in k_{max}, caused by the increase in viscosity, was not largely

affected by temperature. However, the lower heat transfer rates in the xanthan system

were possibly not solely caused by the increased viscosity in comparison to the liquid

system, but also partly by the formation of air bubbles in the xanthan system during

agitation. The presence of an emulsion structure in the model systems (i.e.,

investigated by comparing the xanthan and emulsion 10%) resulted in increased heat

transfer rates.. The effect on k_{max}, however, was strongly dependent on temperature,

with k_{max} being approximately 69% lower in the xanthan system than in the emulsion

10% at 51°C, while k_{max} in the xanthan system was approximately 20% higher than in

the emulsion 10% at 64°C. Finally, an increase in fat content (i.e., emulsion 10% vs. emulsion 20%) did not result in lower heat transfer rates, but k_{max} was significantly lower in the emulsion 20% at temperatures below 59°C. The extent of this effect decreased with increasing temperature, being equal to approximately 99% at 51°C and approximately 21% at 59°C. As mentioned, inactivation kinetics in the emulsion 20% could not be accurately estimated at temperatures higher than 59°C. Hence, the effect of increasing fat content at temperatures above 59°C was not discussed. In conclusion, the effect of food matrix viscosity seems to be closely linked to heat transfer differences, while the effect of food matrix fat content (and the presence of an "emulsion structure") is more complex and largely temperature-dependent. For the effect of fat content, it should also be taken into account that a change in fat content (xanthan vs. emulsion 10% or emulsion 10% vs. emulsion 20%) also entails a change in rheological properties, as shown in Table 4. Therefore, it is not straightforward to isolate the effect of the food matrix fat content on inactivation kinetics.

Since the effect of an increased fat level cannot be explained based on the previous discussion, results from the current study were compared to those obtained at a lab scale at static conditions by Verheyen et al. (2020b). In their study, experiments were conducted in similar emulsion model systems with various fat content (i.e., 1, 5, 10, and 20%) in small glass tubes (i.e., 1 mL of medium) immersed in water baths and involving only a short come-up time of approximately 2 min. At a lab scale, k_{max} decreased with increasing fat content up until a temperature of approximately 59°C (i.e., 0.419, 0.396, 0.339, and 0.322 1/min at 59°C, for systems containing 1, 5, 10, and 20% fat, respectively). However, differences among the different model systems were limited. At higher temperatures, k_{max} in emulsions containing 1, 5, and 20% fat

remained similar (e.g., 2.93, 2.65, and 2.79 1/min, respectively, at 64°C), while k_{max} in

the emulsion containing 10% fat (e.g., 1.96 1/min at 64°C) was significantly lower

than in the other systems. Therefore, the trend of lower k_{max} values in the emulsion

20% than in the emulsion 10% for the Shaka experiments in the current study was

confirmed at a smaller lab scale up until 59°C. Due to the lack of accurate k_{max}

estimations for the emulsion 20% at temperatures higher than 59°C, it was impossible

to determine whether the same trends as for the lab scale also applied for the Shaka at

higher temperatures. Verheyen et al. (2020b) suggested that this trend of decreasing

k_{max} with increasing fat content was caused by differences in thermal conductivity

between the fat and the water phase. The fat droplet size of the emulsion and gelled

emulsion systems in the current study was evenly distributed around 1 µm (Verheyen

et al., 2018) and as the droplets were formed by a shear-based homogenisation at

22,000 rpm, their size was probably not affected by the Shaka agitation. Since the

thermal conductivity of the fat (i.e., sunflower oil) is considerably lower than that of

the water over the relevant temperature range (i.e., 0.168-0.162 and 0.598-0.660

W/(mK), respectively) (Sharqawy, 2013; Turgut et al., 2009), the cells may locally

experience lower temperatures when more fat is present in the model systems. Due to

the agitation during Shaka processing, constantly mixing the model systems, *L.*

monocytogenes cells are often in contact with the fat droplets. Since fat droplet size

remained constant with increasing fat content, the contact time of the cells with the fat

droplets was also longer with increasing fat content, possibly explaining the lower

k_{max} in the emulsion 20% than in the emulsion 10%. At the small scale of the study of

Verheyen et al. (2020b), however, these changes only led to local changes in heat

transfer which resulted in lower k_{max} values seen at some conditions, but did not

directly affect the final *L. monocytogenes* log reductions. Opposite to the effect

observed in the current study, log reductions at the lab-scale were considerably larger

when increasing the fat content from 1 to 5%, but a further increase in fat content did

not result in considerably larger log reductions. In contrast, results from the current

study imply that the aforementioned local differences, although too small to affect the

thermal load values (i.e., as obtained in section 3.2 "Thermal load"), resulted in

significantly smaller *L. monocytogenes* log reductions during Shaka treatments.

4 CONCLUSIONS

This study was one of the first to investigate the effect of food product related properties on bacterial inactivation during a reciprocal agitation thermal process. In comparison to previous studies, the novelty of the current research lies in the use of model food products with compositional and microstructural properties relevant for real food products. Among the different model systems, variations in compositional and physicochemical factors were limited, allowing a systematic investigation of the effect of food matrix rheology and fat content on thermal inactivation of microorganisms.

Food matrix rheology and fat content were demonstrated to exert a significant influence on heat transfer dynamics during Shaka processing. While the effect of food matrix rheology on the inactivation of *L. monocytogenes* could be directly linked to differences in heat transfer dynamics, the situation was more complex for the effect of food matrix fat content. Increasing the fat content from 10 to 20% resulted in a protective environment for the bacterial cells, an effect which was not related to differences in heat transfer dynamics. These phenomena could be troublesome when designing Shaka treatments for food products based solely on measured temperature profiles and theoretical inactivation of pathogens. In future studies, the influence of food product related parameters on heat transfer dynamics in food products during Shaka processing should therefore be studied in parallel with the influence on the thermal inactivation of the foodborne pathogens of interest. In addition, the significant amount of sublethally injured cells following Shaka treatments, as also detected in the

current study, should be taken into account during experimental validation of agitated

retort treatments (e.g., Shaka, end-over-end, and axial rotation) in real food products.

5 ACKNOWLEDGEMENTS

6 REFERENCES

Aryani, D.C., den Besten, H.M.W., Hazeleger, W.C., Zwietering, M.H., 2015. Quantifying variability on thermal resistance of *Listeria monocytogenes*. Int. J. Food Microbiol. 193, 130-138.

Ates, M.B., Skipnes, D., Rode, T.M., Lekang, O.-I., 2014. Comparison of bacterial inactivation with novel agitating retort and static retort after mild heat treatments. Food Control 43, 150-154.

Ates, M.B., Rode, T.M., Skipnes, D., Lekang, O.-I., 2017. Survival of sublethally injured *Listeria* in model soup after nonisothermal heat and high-pressure treatments. Eur. Food Res. Technol. 243, 1083-1090.

Awuah, G.B., Ramaswamy, H.S., Economides, A., 2007. Thermal processing and quality: Principles and overview. Chem. Eng. Process.: Process Intensif. 46, 584-602.

Baka, M., Noriega, E., Van Langendonck, K., Van Impe, J.F., 2016. Influence of food intrinsic complexity on *Listeria monocytogenes* growth in/on vacuum-packed model systems at suboptimal temperatures. Int. J. Food Microbiol. 235, 17-27.

Baka, M., Verheyen, D., Cornette, N., Vercruyssen, S., Van Impe, J.F., 2017. *Salmonella* Typhimurium and *Staphylococcus aureus* dynamics in/on variable (micro)structures of fish-based model systems at suboptimal temperatures. Int. J. Food Microbiol. 240, 32-39.

Ben Embarek, P.K., 1994. Presence, detection and growth of *Listeria monocytogenes* in seafoods: A review. Int. J. Food Microbiol. 23, 17-34.

Berk, Z., 2013. Food Process Engineering and Technology, 2nd edition. Elsevier Inc., Amsterdam (The Netherlands).

Bharti, R.P., Chhabra, R.P., Eswaren, V., 2007. Steady forced convection heat transfer from a heated circular cylinder to power-law fluids. Int. J. Heat Mass Tran. 50, 977-990.

Bharti, R.P., Sivakumar, P., Chhabra, R.P., 2008. Forced convection heat transfer from an elliptical cylinder to power-law fluids. Int. J. Heat Mass Tran. 51, 1838-1853.

Bolton, D.J., McMahon, C.M., Doherty, A.M., Sheridan, J.J., McDowell, D.A., Blair, I.S., Harrington, D., 2000. Thermal inactivation of *Listeria monocytogenes* and *Yersinia enterocolitica* in minced beef under laboratory conditions and in sous-vide prepared minced and solid beef cooked in a commercial retort. J. Appl. Microbiol. 88, 626-632.

Brashears, M.M., Amezquita, A., Stratton, J., 2001. Validation of Methods Used to Recover *Escherichia coli* O157:H7 and *Salmonella* spp. Subjected to Stress Conditions. J. Food Prot. 64(10), 1466-1471.

Busch, S.V., Donnelly C.W., 1992. Development of a repair-enrichment broth for resuscitation of heat-injured *Listeria monocytogenes* and *Listeria innocua*. Appl. Environ. Microbiol. 58, 14-20.

Cariño-Sarabia, A., Vélez-Ruiz, J., 2013. Evaluation of convective heat transfer coefficient between fluids and particles in suspension as food model systems for natural convection using two methodologies. J. Food Process. Eng. 115, 173-181.

Cattani, F., Dolan, K.D., Oliveira, S.D., Mishra, D.K., Ferreira, C.A.S., Periago, P.M., Aznar, A., Fernandez, P.S., Valdramidis, V.P., 2016. One-step global parameter estimation of kinetic inactivation parameters for *Bacillus sporothermodurans* spores under static and dynamic thermal processes. Food Res. Int. 89, 614-619.

Chhabra, A.T., Carter, W.H., Linton, R.H., Cousin, M.A., 1999. A predictive model
to determine the effects of pH, milkfat, and temperature on thermal inactivation
of *Listeria monocytogenes*. J. Food Prot. 62, 1143-1149.

Chhinnan, M.S., McWatters, K.H., Rao, V.N.M., 1985. Rheological characterization
of grain legume pastes and effect of hydration time and water level on apparent
viscosity. J. Food Sci. 50(4), 1167-1171.

Clifcorn, L., Peterson, G., Boyd, J., O'Neil, J., 1950. A new principle for agitating in
processing of canned foods. Food Technol. 4, 450-460.

Datta, A.K., 1993. Error-estimates for approximate kinetic-parameters used in food
literature. J. Food Eng. 18(2), 181-199.

Dwivedi, M., Ramaswamy, H.S., 2010. Comparison of heat transfer rates during
thermal processing under end-over-end and axial modes of rotation. LWT - Food
Sci. Technol. 43, 350-360.

Erdogdu, F., Tutar, M., Øines, S., Barreno, I., Skipnes, D., 2016. Determining the
optimal shaking rate of a reciprocal agitation sterilization systems for liquid
foods: A computational approach with experimental validation. Food Bioprod.
Process. 100, 512-524.

Erdogdu, F., Tutar, M., Sarghini, F., Skipnes, D., 2017. Effects of viscosity and
agitation rate on temperature and flow field in cans during reciprocal agitation. J.
Food Eng. 213, 76-88.

Erdogdu, F., Karatas, O., Sarghini, F., 2018a. A short update on heat transfer
modelling for computational food processing in conventional and innovative
processing. Curr. Opin. Food Sci. 23, 113-119.

Erdogdu, F., Topcam, H., Altin, O., Verheyen, D., Van Impe, J.F., Seow, T.K.,
Skipnes, D., Skåra, T., 2018b. Characterization of fish based model food systems

for microwave heating modeling. In: Van Impe, J., Polanska, M. (Eds.), Proceedings of FOODSIM 2018. EUROSIS-ETI, pp. 235-239.

Fain, Jr., A.R., Line, J.E., Moran, A.B., Martin, L.M., Lechowich, R.V., Carosella, J.M., Brown, W.L., 1991. Lethality of heat to *Listeria monocytogenes* Scott A: D-value and z-value determinations in ground beef and turkey. J. Food Prot. 54, 756-761.

Farber, J.M., Peterkin, P.I., 1991. *Listeria monocytogenes*, a Food-Borne Pathogen. Microbiol. Rev. 55(3), 476-511.

Garre, A., Fernández, P.S., Lindqvist, R., Egea, J.A., 2017. Bioinactivation: Software for modelling dynamic microbial inactivation. Food Res. Int. 93, 66-74.

Geeraerd, A.H., Herremans, C.H., Van Impe, J.F., 2000. Structural model requirements to describe microbial inactivation during a mild heat treatment. Int. J. Food Microbiol. 59, 185-209.

Heertje, I., 2014. Structure and function of food products: A review. Food Struct. 1, 3-23.

Herigstad, B., Hamilton, M., Heersink, J., 2001. How to optimize the drop plate method for enumerating bacteria. J. Microbiol. Methods. 44(2), 121-129.

Juneja, V.K., Eblen, B.S., Marks, H.M., 2001. Modeling non-linear survival curves to calculate thermal inactivation of *Salmonella* in poultry of different fat levels. Int. J. Food Microbiol. 70, 37-51.

Juneja, V.K., Osoria, M., Tiwari, U., Xu, X., Golden, C.E., Mukhopadhyay, S., Mishra, A., 2020. The effect of lauric arginate on the thermal inactivation of starved *Listeria monocytogenes* in *sous-vide* cooked ground beef. Food Res. Int. 134, 109280.

Mackey, B.M., Bratchell, N., 1989. The heat resistance of *Listeria monocytogenes*.

Lett. Appl. Microbiol. 9, 89-94.

Maskan, M., Göğüş, F., 2000. Effect of sugar on the rheological properties of sunflower oil-water emulsions. J. Food Eng. 43, 173-177.

NACMF, 2010. Parameters for determining inoculated pack/challenge study protocols. J. Food Prot. 73(1), 140-202.

Noriega, E., Velliou, E.G., Van Derlinden, E., Mertens, L., Van Impe, J.F., 2013. Effect of cell immobilization on heat-induced sublethal injury of *Escherichia coli*, *Salmonella* Typhimurium and *Listeria innocua*. Food microbiol. 36, 355-364.

Oliveira, R.B.A., Baptista, R.C., Chincha, A.A.I.A., Conceição, D.A., Nascimento, J.S., Costa, L.E.O., Cruz, A.G., Sant'Ana, A.S., 2018. Thermal inactivation kinetics of *Paenibacillus sanguinis* 2301083PRC and *Clostridium sporogenes* JCM1416MGA in full and low fat "requeijão cremoso". Food Control 84, 395-402.

Pratap Singh, A., Ramaswamy, H.S., 2015. Effect of can orientation on heat transfer coefficients associated with liquid particulate mixtures during reciprocating agitation thermal processing. Food Bioprocess. Technol. 8, 1405-1418.

Pratap Singh, A., Ramaswamy, H.S., 2016. Simultaneous optimization of heat transfer and reciprocation intensity for thermal processing of liquid particulate mixtures undergoing reciprocating agitation. Innov. Food Sci. Emerg. Technol. 33, 405-415.

Pratap Singh, A., Singh, A., Ramaswamy, H.S., 2015. Modification of a static steam retort for evaluating heat transfer under reciprocating agitation thermal processing. J. Food Eng. 153, 63-72.

Pratap Singh, A., Singh, A., Ramaswamy, H.S., 2017a. Heat transfer phenomena

during thermal processing of liquid particulate mixtures - a review. Crit. Rev. Food Sci. Nutr. 57(7), 1350-1364.

Pratap Singh, A., Singh, A., Ramaswamy, H.S., 2017b. Using liquid-only cans (equipped with a single particle) to quantify heat transfer phenomenon during thermal processing. Int. J. Food Eng. 13, 20160234.

Pratap Singh, A., Yen, P.P.-L., Ramaswamy, H.S., Singh, A., 2018. Recent advances in agitation thermal processing. Curr. Opin. Food Sci. 23, 90-96.

Ramaswamy, H.S., Marcotte, M., 2005. Food processing: Principles and applications. CRC Press, Boca Raton, FL, USA.

Reiner, M., 1926. Über die Strömung einer elastischen Flüssigkeit durch eine Kapillare. Kolloid Zeitschrift 39, 80-87.

Rosnes, J.T., Skåra, T., Skipnes, D., 2011. Recent advances in minimal heat processing of fish: Effects on microbiological activity and safety. Food Bioprocess. Technol. 4, 833-848.

Sarghini, F., Erdogdu, F., 2016. A computational study on heat transfer characteristics of particulate canned foods during end-over-end rotational agitation: Effect of rotation rate and viscosity. Food Bioprod. Process. 100, 496-511.

Schultze, K.K., Linton, R.H., Cousin, M.A., Luchansky, J.B., Tamplin, M.L., 2007. Effect of preinoculation growth media and fat levels on thermal inactivation of a serotype 4b strain of *Listeria monocytogenes* in frankfurter slurries. Food Microbiol. 24, 352-361.

Sharqawy, M.H., 2013. New correlations for seawater and pure water thermal conductivity at different temperatures and salinities. Desalination 313, 97-104.

Sheridan, P.S., Shilton, N.C., 2002. Determination of the thermal diffusivity of ground beef patties under infrared radiation oven-shelf cooking. J. Food Eng. 52,

39-45.

Singh, A., Ramaswamy, H.S., 2015. Effect of product related parameters on heat-transfer rates to canned particulate non-Newtonian fluids (CMC) during reciprocating agitation thermal processing. J. Food Eng. 165, 1-12.

Skåra, T., Rosnes, J.T., Sivertsvik, M., 2002. Safe and sound: Minimally processed fish products. Food Technology International 2, 75-76.

Smelt, J.P.P.M., Brul, S., 2014. Thermal inactivation of microorganisms. Crit. Rev. Food Sci. Nutr. 54(10), 1371-1385.

Sörqvist, S., 2003. Heat resistance in liquids of *Enterococcus* spp., *Listeria* spp., *Escherichia coli*, *Yersinia enterocolitica*, *Salmonella* spp. and *Campylobacter* spp. Acta Vet. Scand. 44, 1.

Stephens, P.J., Cole, M.R., Jones, M.V., 1994. Effect of heating rate on thermal inactivation of *Listeria monocytogenes*. J. Appl. Bacteriol. 77, 702-708.

Stumbo, C., 1973. Thermobacteriology in Food Processing (2nd ed.). Academic Press (New York, NY, USA).

Sopade, P.A., Filibus, T.E., 1995. The influence of solid and sugar contents on rheological characteristics of akamu, a semi-liquid maize food. J. Food Eng. 24(2), 197-211.

Turgut, A., Tavman, I., Tavman, S., 2009. Measurement of thermal conductivity of edible oils using transient hot wire method. Int. J. Food Prop. 12(4), 741-747.

Valdramidis, V.P., Geeraerd, A.H., Bernaerts, K., Van Impe, J.F., 2006a. Microbial dynamics versus mathematical model dynamics: the case of microbial heat resistance induction. Innov. Food Sci. Emerg. Technol. 7, 118-125.

Valdramidis, V.P., Geeraerd, A.H., Gaze, J.E., Kondjoyan, A., Boyd, A.R., Shaw, H.L., Van Impe, J.F., 2006b. Quantitative description of *Listeria monocytogenes*

inactivation kinetics with temperature and water activity as the influencing factors; model prediction and methodological validation on dynamic data. J. Food Eng. 76, 79-88.

Valdramidis, V.P., Geeraerd, A.H., Van Impe, J.F., 2007. Stress-adaptive responses by heat under the microscope of predictive microbiology. J. Appl. Microbiol. 103, 1922-1930.

Valdramidis, V.P., Geeraerd, A.H., Bernaerts, K., Van Impe, J.F.M., 2008. Identification of non-linear microbial inactivation kinetics under dynamic conditions. Int. J. Food Microbiol. 128, 146-152.

Van Netten, P., Perales, I., van de Moosdijk, A., Curtis, G.D.W., Mossel, D.A.A., 1989. Liquid and solid selective differential media for the detection and enumeration of *L. monocytogenes* and other *Listeria* spp. Int. J. Food Microbiol. 8, 299–316.

Velliou, E.G., Noriega, E., Van Derlinden, E., Mertens, L., Boons, K., Geeraerd, A.H., Devlieghere, F., Van Impe, J.F., 2013. The effect of colony formation on the heat inactivation dynamics of *Escherichia coli* K12 and *Salmonella* typhimurium. Food Res. Int. 54(2), 1746-1752.

Verheyen, D., Baka, M., Glorieux, S., Duquenne, B., Fraeye, I., Skåra, T., Van Impe, J.F., 2018. Development of fish-based model systems with various microstructures. Food Res. Int., 106, 1069-1076.

Verheyen, D., Baka, M., Akkermans, S., Skåra, T., Van Impe, J.F., 2019. Effect of microstructure and initial cell conditions on thermal inactivation kinetics and sublethal injury of *Listeria monocytogenes* in fish-based food model systems. Food Microbiol. 84, 103267.

Verheyen, D., Bolívar, A., Pérez-Rodríguez, F., Baka, M., Skåra, T., Van Impe, J.F.,

2020a. Isolating the effect of fat content on *Listeria monocytogenes* growth dynamics in fish-based emulsion and gelled emulsion systems. Food Control 108, 106874.

Verheyen, D., Govaert, M., Seow, T.K., Ruvina, J., Mukherjee, V., Baka, M., Skåra, T., Van Impe, J.F., 2020b. The complex effect of food matrix fat content on thermal inactivation of *Listeria monocytogenes*: Case study in emulsion and gelled emulsion model systems. Front. Microbiol. 10, 3149.

Vitali, A.A., Rao, M.A., 1984. Flow properties of low-pulp concentrated orange juices: effect of temperature and concentration. J. Food Sci. 49(3), 882-888.

Walden, R., Emanuel, J., 2010. Developments in in-container retort technology: the Zinetec Shaka process. In Doona, C.J., Kustin, K., Feeherry, F.E. (Eds.). Case studies in novel food processing technologies: Innoviation in processing, packaging, and predictive modeling. Woodhead Publishing Ltd., Cambridge, UK, pp. 359-406.

Wedding, L.M., Balestrini, C.G., Shafer, B.D., 2007. Canned Foods: Principles of thermal process control, Acidification and container closure evaluation (seventh ed.). GMA Science and Education Foundation, Washington D.C. (US).

Wilson, P.D.G., Brocklehurst, T.F., Arino, S., Thuault, D., Jakobsen, M., Lange, M., Farkas, J., Wimpenny, J.W.T., Van Impe, J.F., 2002. Modelling microbial growth in structured foods: towards a unified approach. Int. J. Food Microbiol. 73, 275-289.

TABLES

Table 1: Composition (% w/w) of the four different model systems, i.e., liquid, xanthan, the emulsion 10% fat (em10), and the emulsion 20% (em20).

Ingredient	Liquid[1]	Xanthan[1]	em10[2]	em20[2]
Protein (ProGo[TM], Hofseth Biocare ASA, Ålesund, Norway)	5.00	5.00	5.00	5.00
Sodium Alginate (Sigma-Aldrich, MO, USA)	3.00	3.00	3.00	3.00
NaCl (Sigma-Aldrich, MO, USA)	0.96	0.96	0.84	0.74
Sunflower oil (Eldorado, local supermarket, Stavanger, Norway)	/	/	10.00	20.00
Tween 80 (Sigma-Aldrich, MO, USA)	/	/	0.35	0.35
Span 80 (Sigma-Aldrich, MO, USA)	/	/	0.65	0.65
Xanthan gum (Sigma-Aldrich, MO, USA)	/	0.50	0.50	0.50
Distilled H_2O	91.04	90.54	79.66	69.76

[1]Composition provided by Verheyen et al. (2018)

[2]Composition provided by Verheyen et al. (2020a)

Table 2: Shaka inactivation process steps. The holding phase temperature (T_h) and holding phase time (t_h) are dependent on the specific inactivation process.

Phase	Time$_a$ (min)	Retort water temperature (°C)	Agitation rate (spm)	Overpressure (bar)
Filling	2	20-42	0	0.4
Heating	2	42-T_h	80	0.4
Holding	t_h	T_h	100	0.4
Cooling 1	3-4	T_h-30	100	0.3
Cooling 2	5	30-20	80	0.2

$_a$Approximate times are provided, since slight variations might occur during the different processes

Table 3: Treatment duration of the different Shaka inactivation processes at each temperature (holding phase temperature). At each temperature, a short (t_1), intermediate (t_2), and long (t_3) treatment duration were selected.

Temperature (°C)	t_1 (min)		t_2 (min)		t_3 (min)	
	Holding time	Total time$_a$	Holding time	Total time$_a$	Holding time	Total time$_a$
59	22.5	32.9	32.5	42.9	37.5	47.9
64	10.4	21.5	12.0	22.8	13.4	24.0
69	7.3	18.4	8.1	19.3	8.8	20.1

$_a$Approximate total times are provided, since slight variations might occur during the different processes

Table 4: Rheological parameters of the liquid (liq), xanthan (xan), emulsion 10% (em10) and emulsion 20% (em20) systems, according to the power law model (Reiner, 1926), i.e., the consistency index *K* and the flow behaviour index *n*. For the different model systems at one temperature, values bearing different uppercase letters are significantly different (P ≤ 0.05).

T (°C)	K (Pa/s)				n (-)			
	liq	xan	em10[1]	em20[1]	liq	xan	em10[1]	em20[1]
20.0°C	0.118 ± 0.001^A	1.486 ± 0.291^B	1.786 ± 0.017^B	5.477 ± 0.528^C	0.963 ± 0.003^C	0.626 ± 0.047^B	0.646 ± 0.002^B	0.528 ± 0.019^A
32.5°C	0.087 ± 0.004^A	1.138 ± 0.186^B	1.529 ± 0.090^B	4.243 ± 0.573^C	0.961 ± 0.011^C	0.645 ± 0.029^B	0.653 ± 0.003^B	0.512 ± 0.007^A
45.0°C	0.057 ± 0.002^A	0.773 ± 0.202^{AB}	1.226 ± 0.226^B	3.631 ± 0.671^C	0.972 ± 0.001^C	0.671 ± 0.054^B	0.655 ± 0.001^B	0.491 ± 0.015^A
57.5°C	0.052 ± 0.002^A	0.530 ± 0.176^B	1.111 ± 0.126^C	2.993 ± 0.262^D	0.960 ± 0.014^C	0.707 ± 0.050^B	0.649 ± 0.032^B	0.489 ± 0.017^A
70.0°C	0.047 ± 0.003^A	0.285 ± 0.035^B	0.973 ± 0.026^C	1.937 ± 0.082^D	0.847 ± 0.030^C	0.716 ± 0.044^B	0.619 ± 0.009^A	0.554 ± 0.002^A

[1]Rheological parameters provided by Verheyen et al. (2020b)

Table 5: Thermal load (°C·min) to which the cells were exposed during the different Shaka treatments. Shaka treatments are identified based on their holding phase (i.e., temperature and time). For the different model systems at one temperature and treatment time, values bearing different uppercase letters are significantly different (P ≤ 0.05).

T (°C)	Time (min)	Model systems			
		liquid	xanthan	em10	em20
59	22.5	1287 ± 7^C	1244 ± 9^A	1259 ± 4^{AB}	1268 ± 5^B
	32.5	1883 ± 7^C	1838 ± 9^A	1854 ± 5^{AB}	1864 ± 5^B
	37.5	2179 ± 7^C	2133 ± 8^A	2151 ± 5^B	2161 ± 5^B
64	10.4	634 ± 3^C	576 ± 8^A	607 ± 11^B	568 ± 7^A
	12.0	698 ± 6^B	650 ± 12^A	696 ± 10^B	691 ± 11^B
	13.4	794 ± 4^B	746 ± 7^A	795 ± 3^B	791 ± 6^B
69	7.1	428 ± 9^B	397 ± 2^A	443 ± 5^B	444 ± 6^B
	8.1	512 ± 7^B	478 ± 12^A	504 ± 4^B	498 ± 3^{AB}
	8.8	567 ± 4^C	510 ± 4^A	541 ± 12^B	547 ± 13^{BC}

Table 6: Log reductions of *Listeria monocytogenes* in the model systems following the different Shaka treatments. Shaka treatments are identified based on their holding phase (i.e., temperature and time). For the different model systems per treatment, values bearing different uppercase letters are significantly different (P ≤ 0.05).

T (°C)	Time (min)	Model systems			
		liquid	xanthan	em10	em20
59	22.5	2.1 ± 0.8^{B}	1.4 ± 0.5^{AB}	1.4 ± 0.4^{AB}	0.5 ± 0.5^{A}
	32.5	4.4 ± 0.1^{B}	3.0 ± 0.8^{AB}	4.7 ± 1.6^{B}	2.2 ± 0.3^{A}
	37.5	5.7 ± 0.6^{B}	2.7 ± 0.9^{A}	6.0 ± 0.3^{B}	3.9 ± 1.2^{A}
64	10.4	2.2 ± 1.6^{A}	0.6 ± 0.2^{A}	0.7 ± 0.6^{A}	0.1 ± 0.3^{A}
	12.0	1.8 ± 1.5^{A}	1.4 ± 0.9^{A}	1.3 ± 0.6^{A}	0.2 ± 0.4^{A}
	13.4	$5.8\pm2.2^{B}_{1}$	1.2 ± 1.0^{A}	2.4 ± 1.2^{A}	0.9 ± 0.6^{A}
69	7.1	3.8 ± 2.8^{B}	0.4 ± 0.2^{A}	0.8 ± 0.5^{A}	0.1 ± 0.3^{A}
	8.1	5.5 ± 0.5^{C}	0.8 ± 0.5^{AB}	1.1 ± 0.5^{B}	0.1 ± 0.3^{A}
	8.8	$6.2\pm1.5^{C}_{1}$	1.4 ± 0.6^{AB}	2.4 ± 1.5^{B}	0.2 ± 0.4^{A}

$_{1}$Counts were below the detection limit for at least one of the replicates

Table 7: Sublethal injury (%) of *Listeria monocytogenes* following the different Shaka treatments. Shaka treatments are identified based on their holding phase (i.e., temperature and time). For the different model systems per treatment, values bearing different uppercase letters are significantly different (P ≤ 0.05).

T (°C)	Time (min)	Model systems			
		liquid	xanthan	em10	em20
59	22.5	67 ± 21^A	79 ± 15^A	74 ± 11^A	46 ± 27^A
	32.5	97 ± 3.2^C	71 ± 3^A	$91\pm3^{BC}_1$	86 ± 7^B
	37.5	91 ± 11^A_1	80 ± 8^A	95 ± 5^A_1	87 ± 7^A
64	10.4	71 ± 41^B	11 ± 2^A	30 ± 33^{AB}	23 ± 22^{AB}
	12.0	59 ± 42^A	26 ± 8^A	66 ± 21^A	32 ± 39^A
	13.4	99 ± 0.3^B_1	32 ± 37^A	92 ± 3^B	49 ± 4^A
69	7.1	$55\pm29^{AB}_1$	16 ± 15^A	68 ± 28^B	17 ± 21^A
	8.1	71 ± 41^B_1	28 ± 7^A	8 ± 14^A	3 ± 6^A
	8.8	$58\pm59^{AB}_1$	27 ± 46^{AB}	86 ± 12^B	11 ± 7^A

$_1$counts below the detection limit (DL) on PALCAM for at least one of the replicates

Table 8: Estimated parameters (± SD) and mean squared error (MSE) of the Geeraerd et al. (2000) model for the inactivation of *L. monocytogenes* in the different model systems over the course of the Shaka treatments (for the treatments with the longest holding time at each temperature). For each model system, the differential equations of the model were solved simultaneously for the inactivation data at 59, 64, and 69°C, using a reference temperature T_{ref} of 59°C. Estimates for the following parameters are provided: the maximum specific inactivation rate at the reference temperature $k_{max}(T_{ref})$, the residual cell population N_{res} at each of the three temperatures (i.e., 59, 64, and 69°C), and the z-value. For the different model systems, values bearing different uppercase letters are significantly different (P ≤ 0.05).

	liquid	xanthan	em10	em20
$k_{max}(T_{ref})$ (1/min)	0.189±0.003[C]	0.131±0.001[A]	0.179±0.003[B]	0.124±0.027[A]
log N_{res}(59°C) (log CFU/mL)	2.68±0.01[A]	5.85±0.01[D]	3.10±0.01[B]	4.89±0.89[C]
log N_{res}(64°C) (log CFU/mL)	4.50±0.01[A]	7.44±0.01[C]	6.32±0.03[B]	7.90±0.45[D]
log N_{res}(69°C) (log CFU/mL)	2.52±0.01[A]	7.06±0.01[C]	5.95±0.02[B]	8.25±0.01[D]
z (°C)	7.71±0.02[B]	8.22±0.01[C]	13.38±0.03[D]	1.20±0.01[A]
MSE (-)	7.28	1.28	3.44	1.58

FIGURE CAPTIONS

Figure 1: Schematic overview of the Shaka agitated retort system.

Figure 2: Temperature evolution over the course of the Shaka experiments with a holding temperature of 69°C inside the different model systems, i.e., liquid (A), xanthan (B), emulsion 10% (C), and emulsion 20% (D). The retort water temperature for each of the treatments is indicated by the respective dashed lines.

Figure 3: Estimated thermal inactivation of *Listeria monocytogenes* during Shaka processes with a holding temperature and time of 59°C and 37.5 min inside the different model systems, i.e., liquid (A), xanthan (B), emulsion 10% (C), and emulsion 20% (D). Symbols correspond to the transformed data used for the model fit (x). Black lines correspond to the fit of the Geeraerd et al. (2000) model to the experimental data. Blue lines correspond to the temperature recorded inside the model system during the treatment. De detection limit (DL) is also shown on the graphs.

Figure 4: Estimated thermal inactivation of *Listeria monocytogenes* during Shaka processes with a holding temperature and time of 64°C and 13.4 min inside the different model systems, i.e., liquid (A), xanthan (B), emulsion 10% (C), and emulsion 20% (D). Symbols correspond to the transformed data used for the model fit (x). Black lines correspond to the fit of the Geeraerd et al. (2000) model to the experimental data. Blue lines correspond to the temperature recorded inside the model system during the treatment. De detection limit (DL) is also shown on the graphs.

Figure 5: Estimated thermal inactivation of *Listeria monocytogenes* during Shaka processes with a holding temperature and time of 69°C and 8.8 min inside the different model systems, i.e., liquid (A), xanthan (B), emulsion 10% (C), and emulsion 20% (D). Symbols correspond to the transformed data used for the model fit (x). Black lines correspond to the fit of the Geeraerd et al. (2000) model to the experimental data. Blue lines correspond to the temperature recorded inside the model system during the treatment. De detection limit (DL) is also shown on the graphs.

Figure 6: Temperature-dependency of the maximum specific inactivation rate k_{max}, based on the model of Geeraerd et al. (2000), for the inactivation of *Listeria monocytogenes* in the different model systems. For the emulsion 20%, k_{max} values above 59°C are represented with a dashed line, since model predictions were not accurate over this temperature range.

SUPPLEMENTARY MATERIAL

Supplementary material 1: Physicochemical properties of the four different model systems, i.e., liquid, xanthan, emulsion 10% fat (em10), and emulsion 20% fat (em20).


Supplementary material 2: Temperature evolution over the course of the Shaka experiments with a holding temperature of 59°C inside the different model systems, i.e., liquid (A), xanthan (B), emulsion 10% (C), and emulsion 20% (D). The retort water temperature for each of the treatments is indicated by the respective dashed lines.


Supplementary material 3: Temperature evolution over the course of the Shaka experiments with a holding temperature of 64°C inside the different model systems, i.e., liquid (A), xanthan (B), emulsion 10% (C), and emulsion 20% (D). The retort water temperature for each of the treatments is indicated by the respective dashed lines.
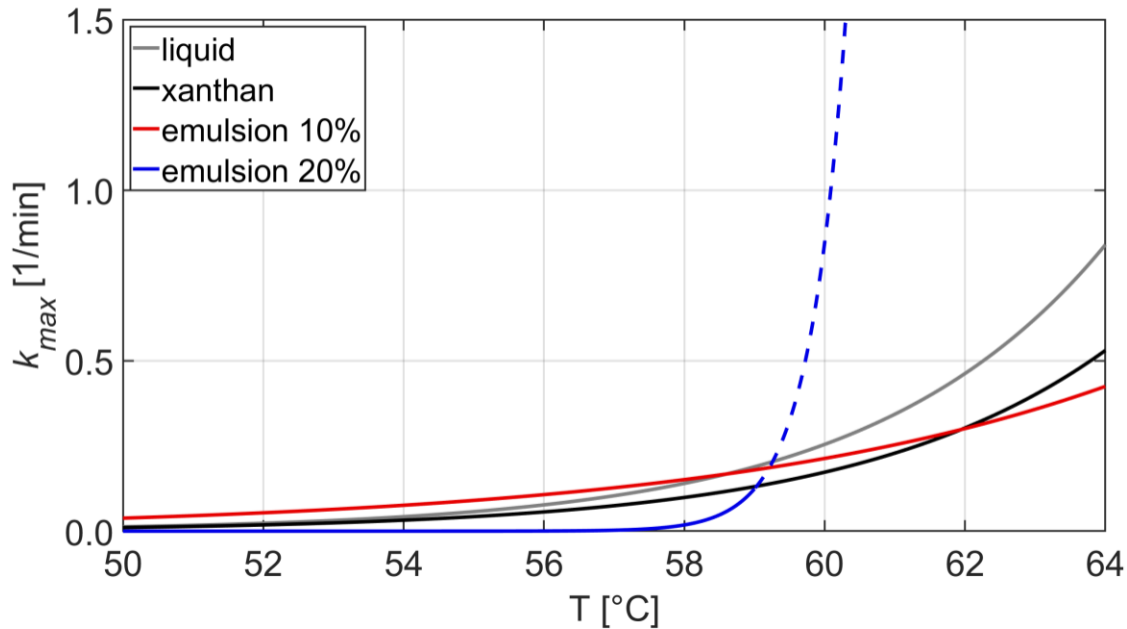
Steam

Preheating tank

SHAKA

Pressurized air

Cooling water

Circulation pump
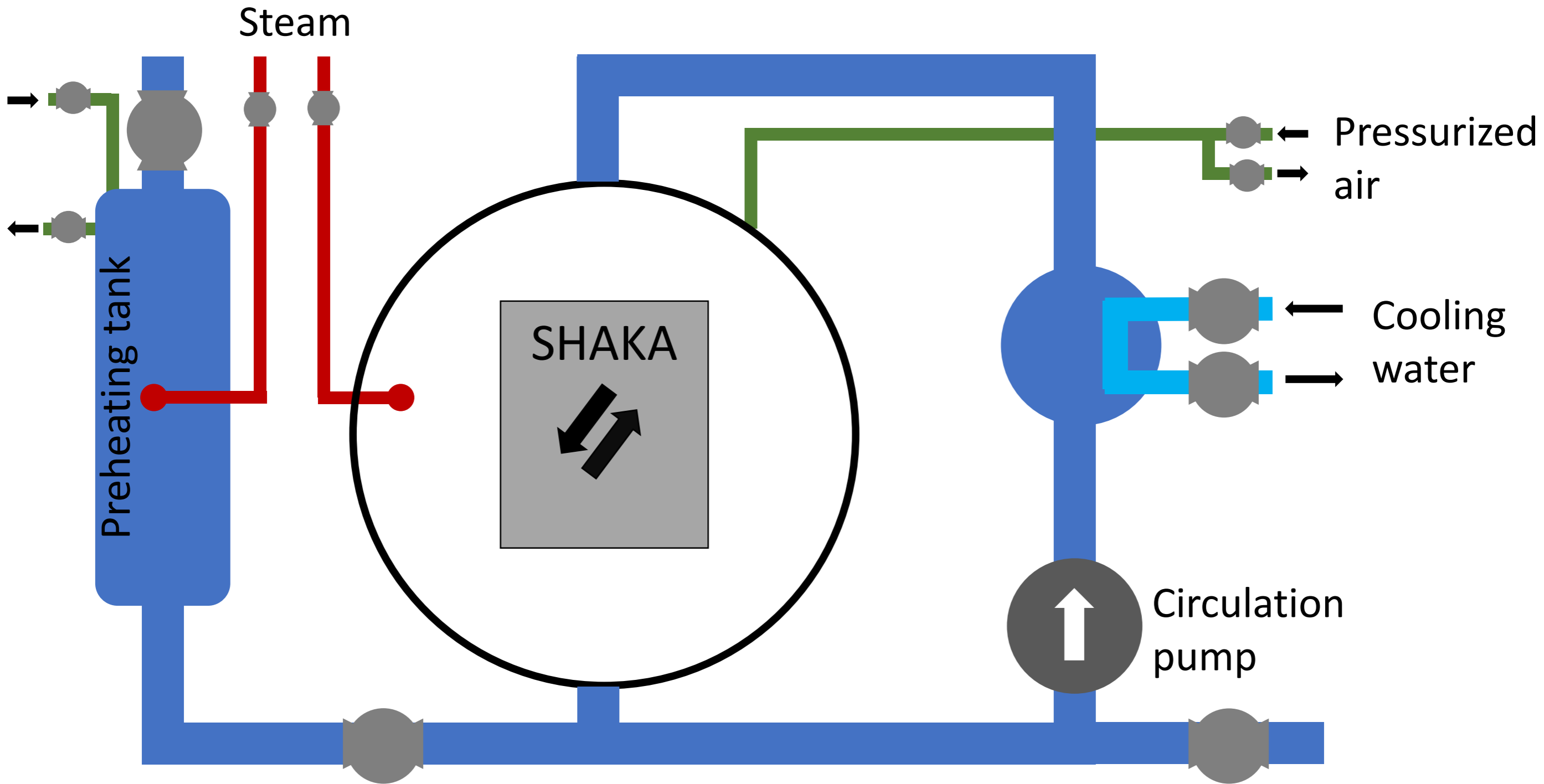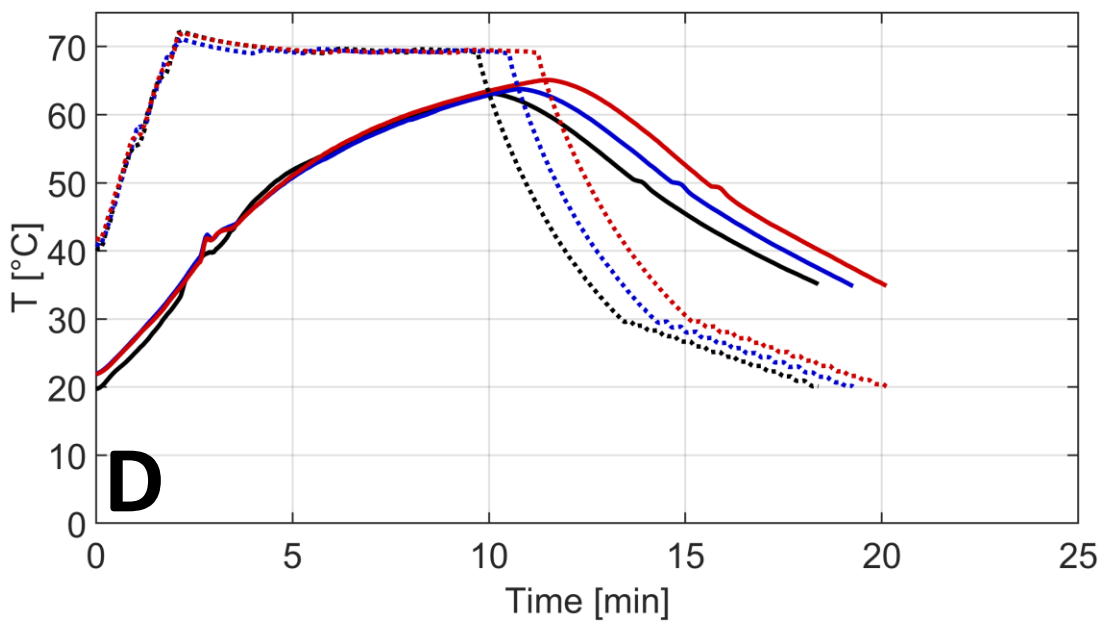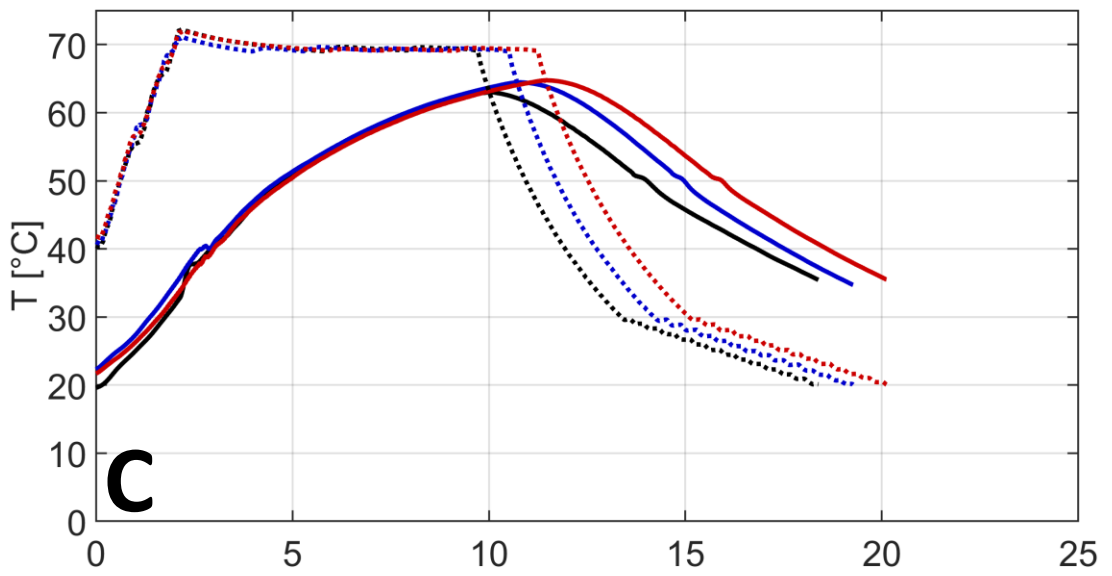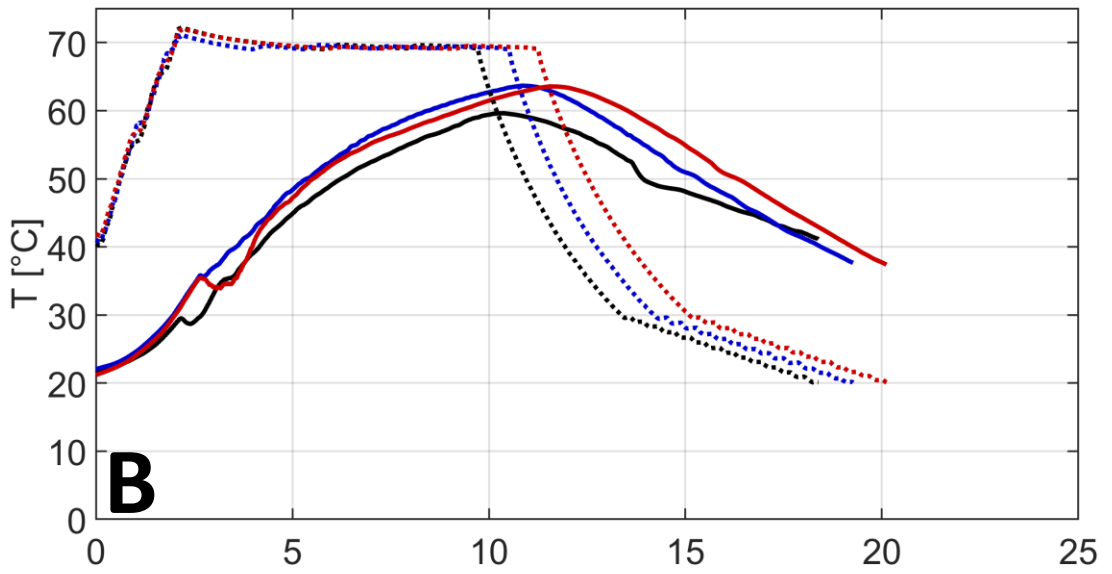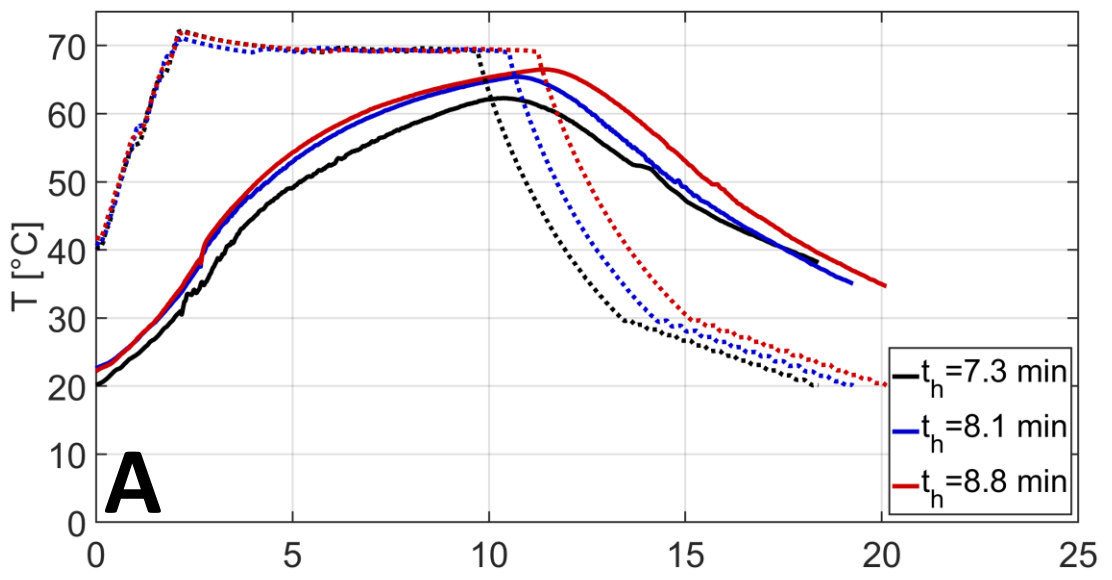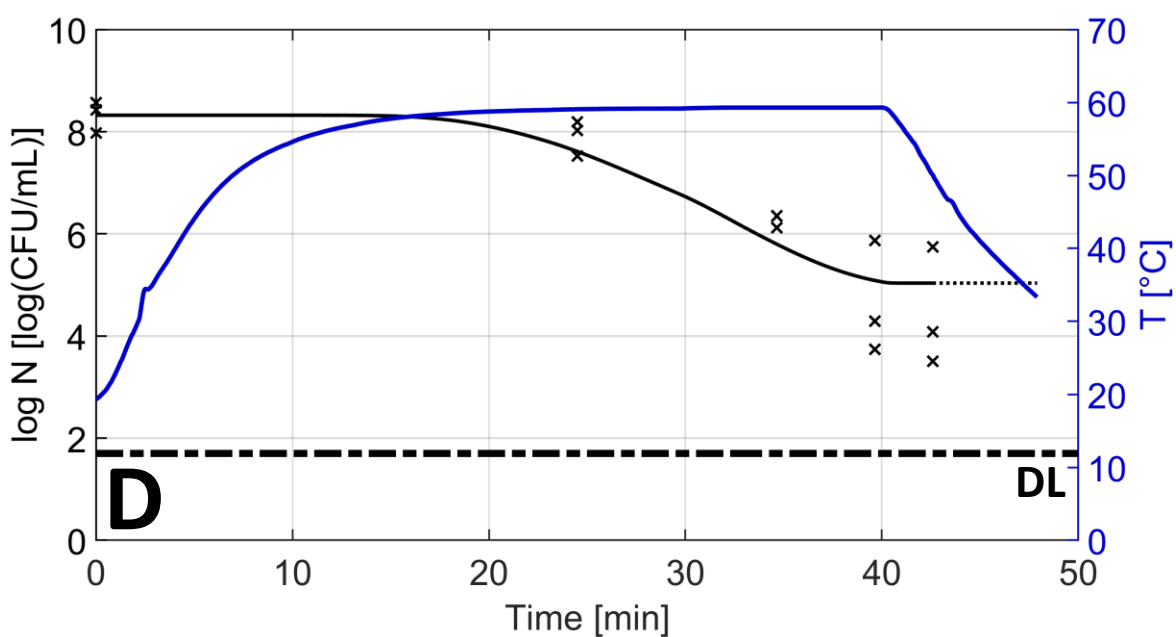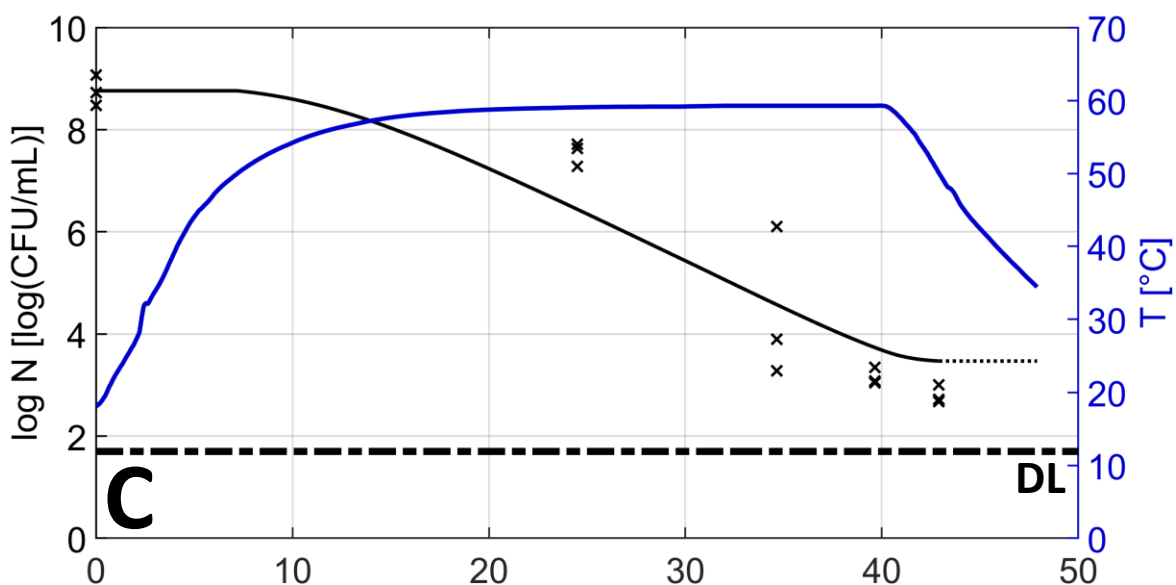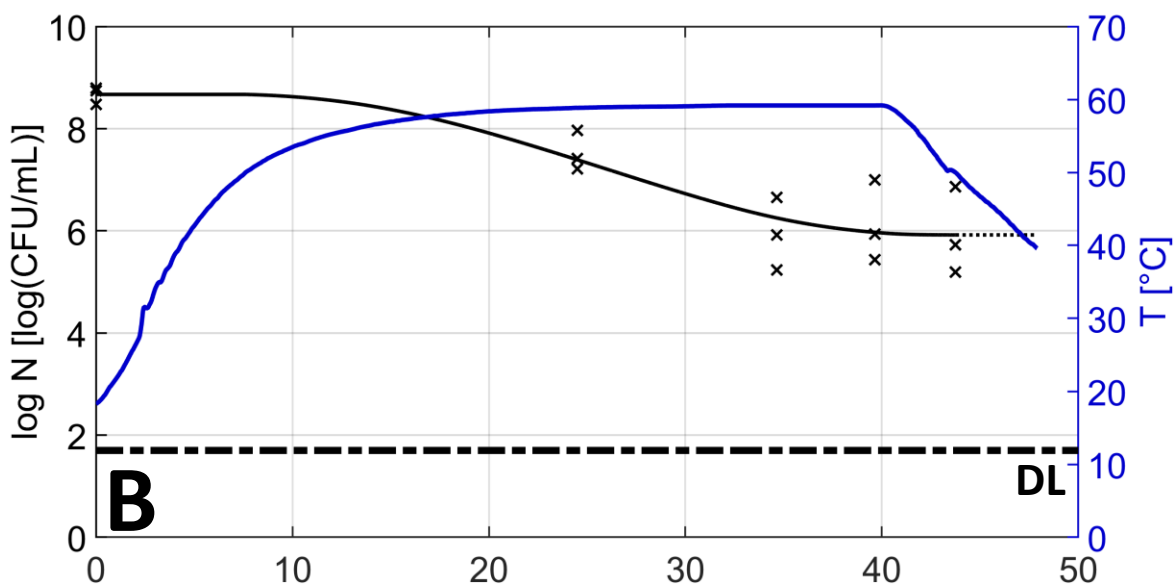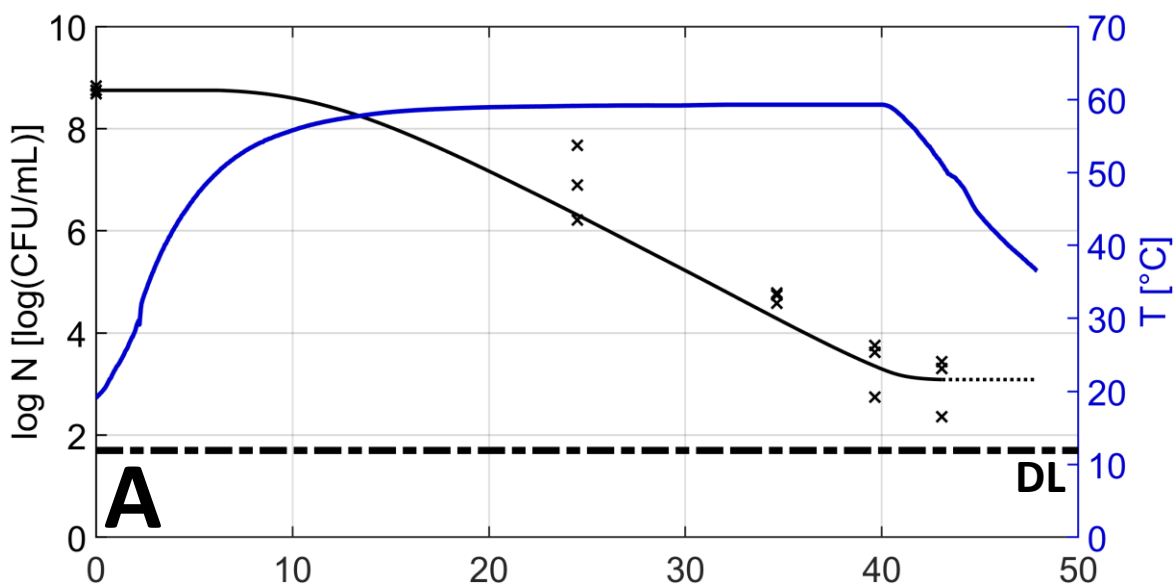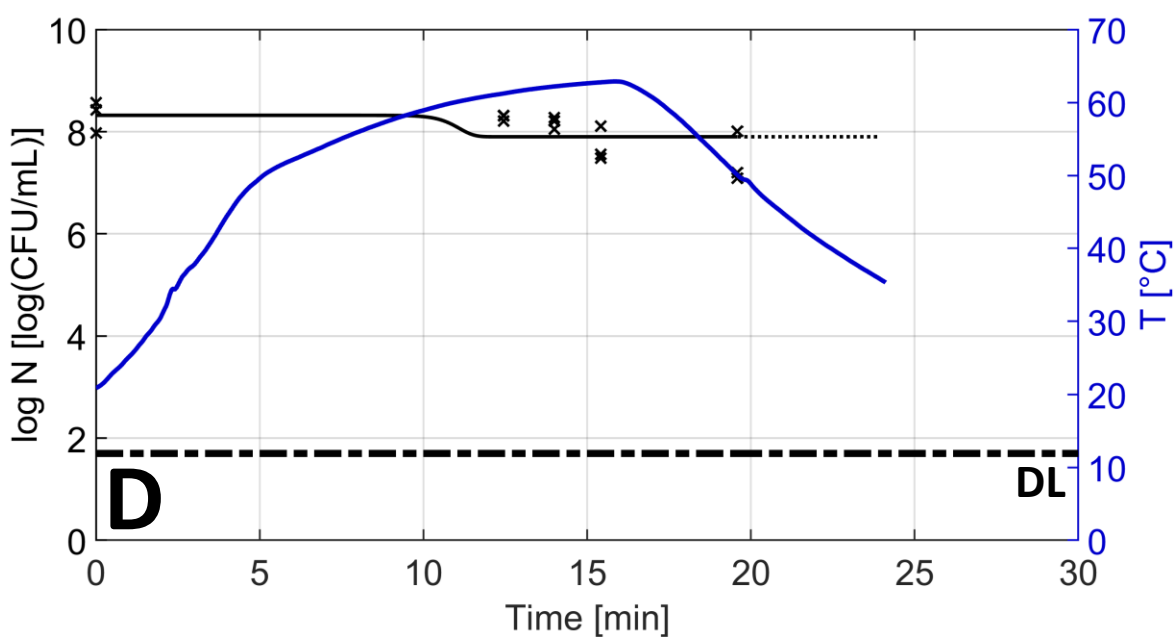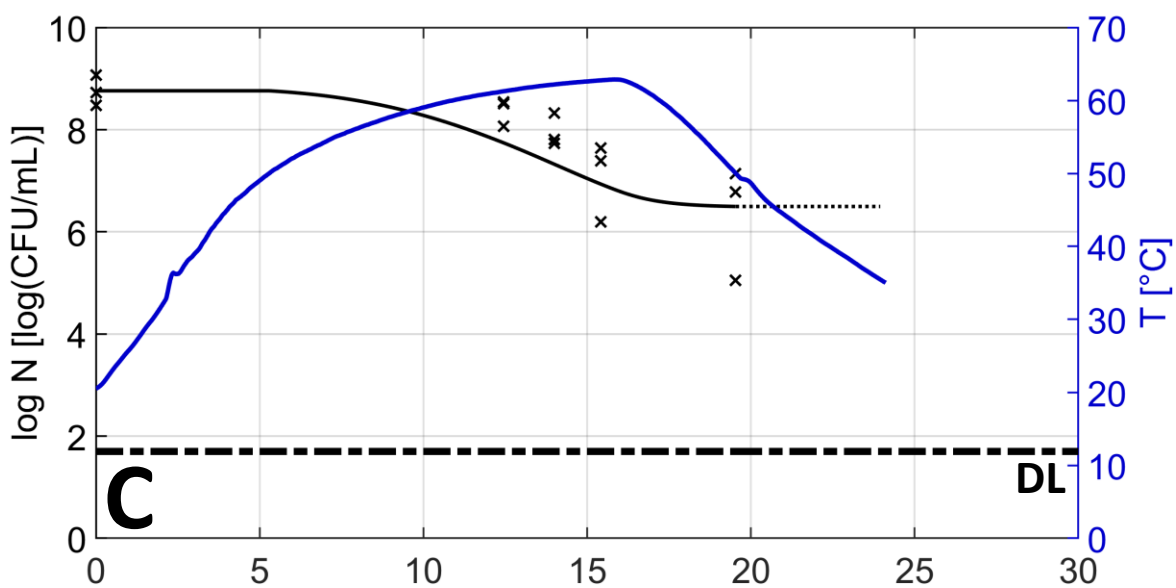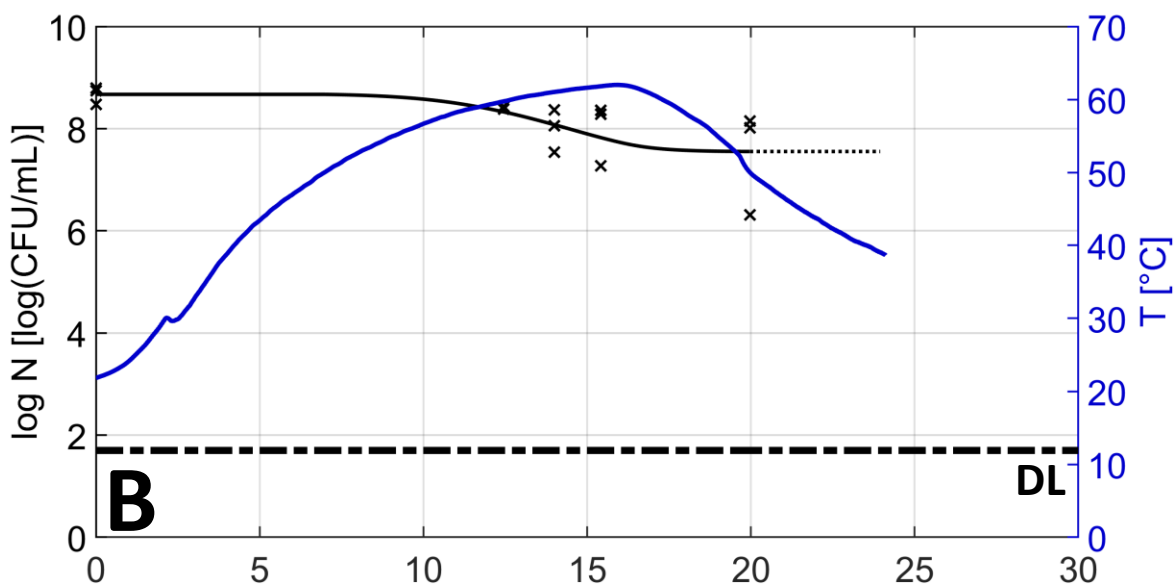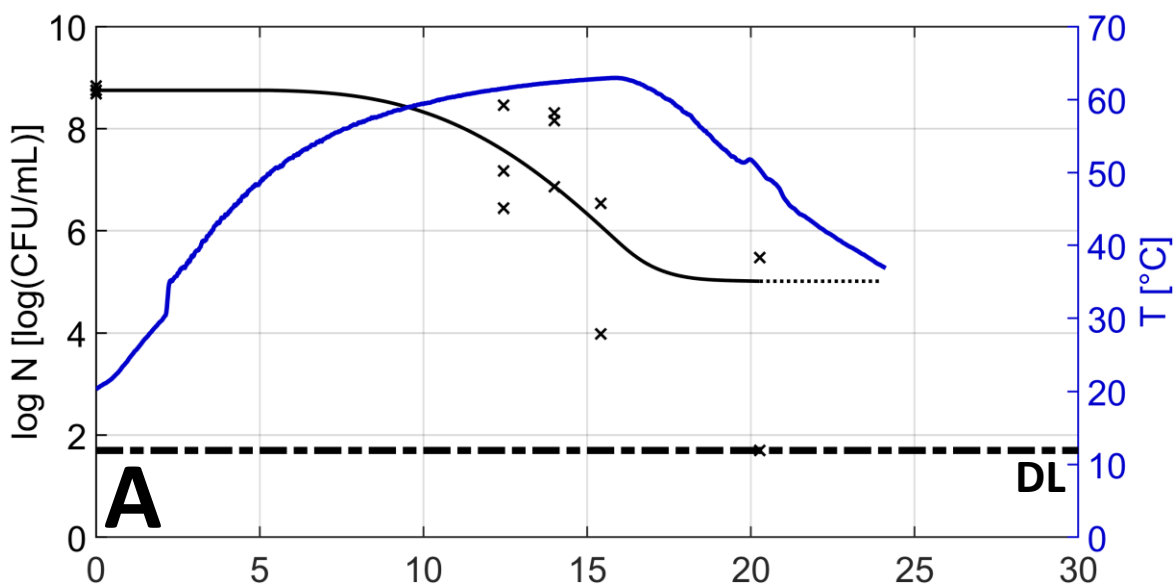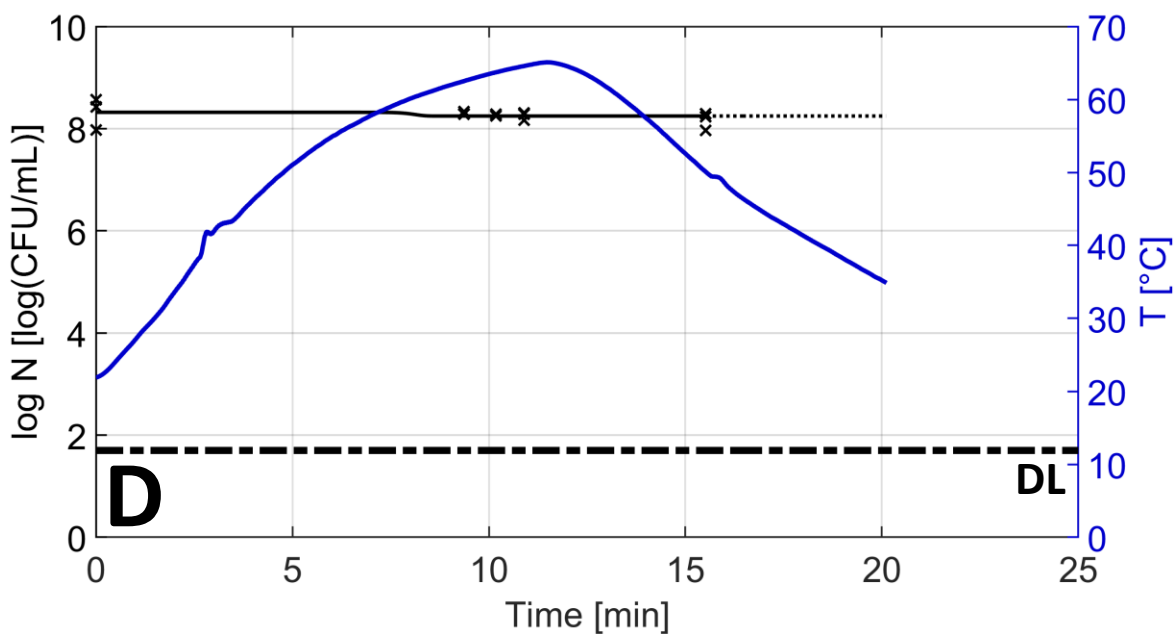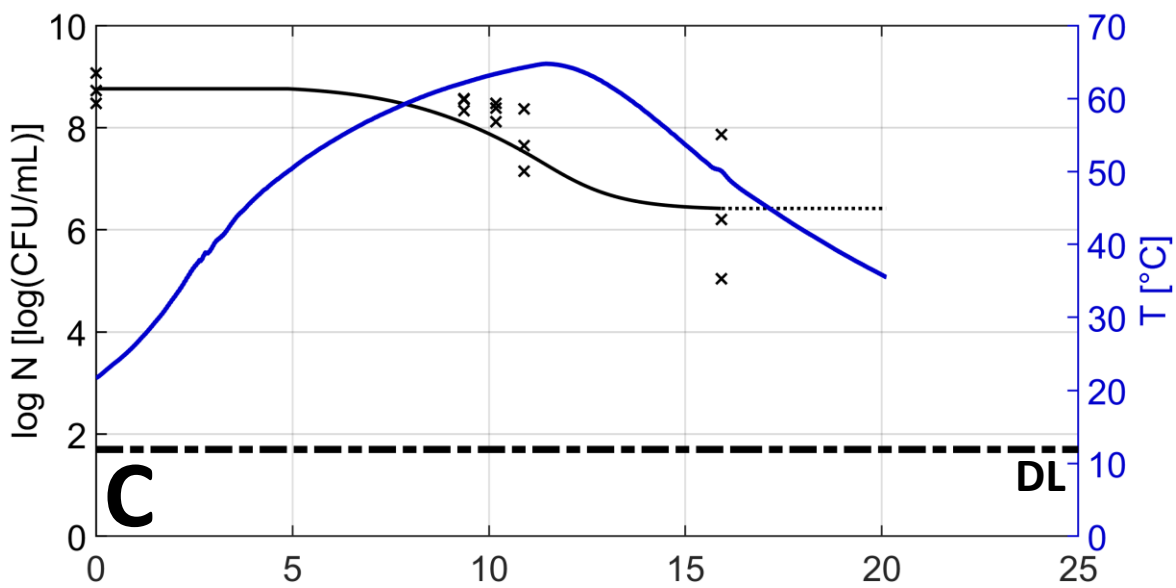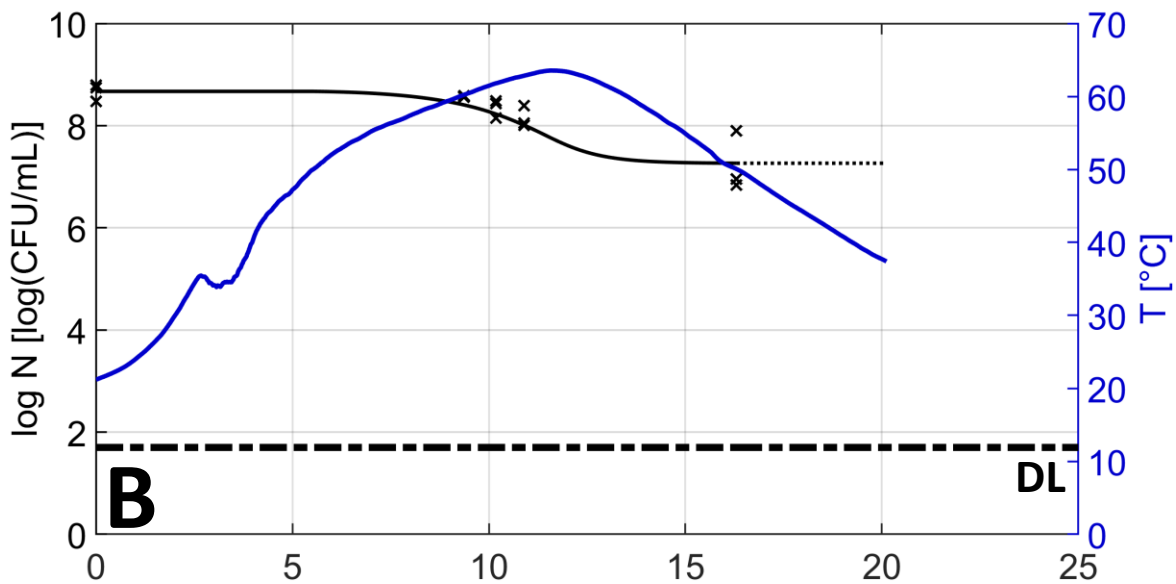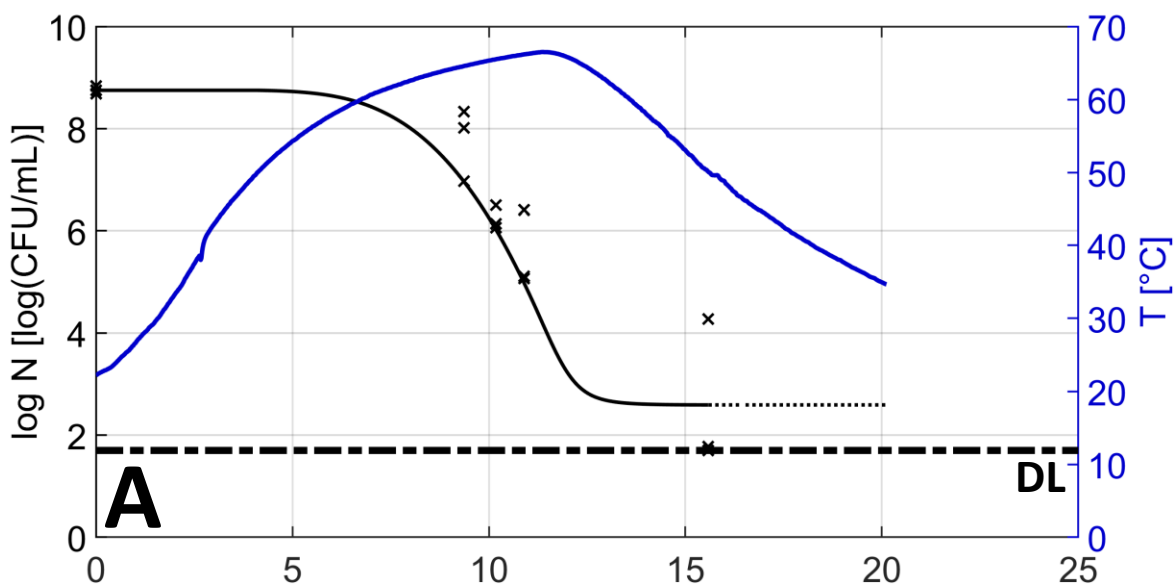
	liquid[1]	xanthan[1]	em10[2]	em20[2]
Density (kg/m^3)	1033±2	1037±1	1011±2	978±8
pH (-)	6.36±0.16	6.34±0.01	6.15±0.06	6.19±0.08
a_w (-)	0.989±0.001	0.987±0.002	0.990±0.003	0.989±0.002

[1]pH and a_w provided by Verheyen et al. (2018)

[2]pH and a_w provided by Verheyen et al. (2020a)